Ore Geology Reviews 150 (2022) 105126

Contents lists available at ScienceDirect

Ore Geology Reviews

journal homepage: www.elsevier.com/locate/oregeorev

# Petrological and geochemical characteristics of the mafic–ultramafic Americano do Brasil Complex, central Brazil, and the implications for its genesis

Cláudia T. Augustin [a,b,*], James E. Mungall [a], Maria E. Schutesky [b], Richard Ernst [a,c], Victor B. Garcia [d]

[a] Mineral Deposits Laboratory, Department of Earth Science, Carleton University, 2115 Herzberg Laboratories, 1125 Colonel By Dr., Ottawa, ON K1S 5B6, Canada
[b] Instituto de Geociências, Universidade de Brasília, Brasília, DF 70910-900, Brazil
[c] Faculty of Geology and Geography, Tomsk State University, Tomsk, Russia
[d] Department of Earth and Environmental Sciences, University of Ottawa, Advanced Research Complex, 25 Templeton Street, Ottawa, ON K1N 6N5, Canada

ARTICLE INFO

*Keywords:*
Geochemistry
Igneous petrology
Mafic–ultramafic intrusion
Brasilia belt

ABSTRACT

The Americano do Brasil Complex occurs in the Neoproterozoic Goias Magmatic Arc, central Brazil. It is composed of two mafic–ultramafic cumulate sequences, intruded into granodioritic gneisses. Although deformed and partially recrystallized by a regional metamorphic overprint, the complex still preserves relict igneous features, such as adcumulate to heteradcumulate textures. The Northern sequence is mostly composed of olivine and olivine-clinopyroxene cumulates, whereas the Southern consists mainly of two-pyroxene cumulate rocks, with plagioclase and olivine cumulates occurring in lesser amounts. The complex has three main orebodies, with textures that range from disseminated to massive sulfide breccias with durchbewegung texture. Thermodynamic modeling using a single picrite parental magma composition can predict cumulate rock compositions and mineral modes similar to all of the observed cumulate rock compositions of the Americano do Brasil Complex. Equilibrium crystallization of the liquid and assimilation-batch-crystallization involving up to 45 % of the host gneisses in the upper crust produces solids similar to the cumulates described in the Northern and Southern sequences, respectively. Modeled pressure–temperature emplacement conditions of the magma were c.a. 2.5 kbar and 1310 °C. Both sequences have similar incompatible trace element patterns which, together with the results of the modeling, imply a broadly comagmatic origin.

## 1. Introduction

Magmatic Ni–Cu sulfide deposits are most commonly known to be hosted by mafic to ultramafic intrusions and can occur in a variety of tectonic settings. Until recently, exploration for world-class Ni-Cu-(PGE) deposits has focused on extensional tectonic environments, such as ancient rift basins, and convergent margins have not been seen as viable target areas for magmatic sulfide-rich Ni-Cu-(PGE) deposits (Ripley, 2010). In the past two decades, however, several mineralized mafic–ultramafic intrusions located in accretive or collisional tectonic settings have been studied showing an increasing resource variety and new important exploration targets. Notable examples are Aguablanca (e.g. Piña, 2019) in Spain; the intrusions in Portneuf-Mauricie Domain (e.g. Sappin et al., 2009), and the Giant Mascot Suite (Manor et al., 2016), in Canada; the Savannah Ni-Cu-Co Camp in the East Kimberley (e.g. Le Vaillant et al. (2020), in Australia; the Limoeiro (e.g. Mota-E-Silva et al., 2013) and Mirabela Intrusions (e.g. Barnes et al., 2011) in Brazil; and the Ntaka Hill intrusion in Tanzania (Barnes et al., 2019). In these compressive environments, the mafic–ultramafic intrusions have been correlated to a variety of sources and pathways for magma generation and emplacement. A few intrusions located in orogenic environments are interpreted to be pre-orogenic, but most of them are interpreted to be syn-collisional, commonly related to cumulates of magmatic arc roots or even back-arc basins, and some can be related to post-orogenic settings, commonly linked to mantle plumes and/or LIPs (e.g. Barnes et al., 2019; Le Vaillant et al. 2020; Maier et al., 2008; Piña, 2019; Sappin et al.,

* Corresponding author at: Mineral Deposits Laboratory, Department of Earth Science, Carleton University, 2115 Herzberg Laboratories, 1125 Colonel By Dr., Ottawa, ON K1S 5B6, Canada.
*E-mail address:* claudia.augustin@carleton.ca (C.T. Augustin).

https://doi.org/10.1016/j.oregeorev.2022.105126
Received 12 February 2022; Received in revised form 23 September 2022; Accepted 25 September 2022
Available online 26 September 2022

2012).

The Americano do Brasil Complex is part of a group of mafic–ultramafic intrusions occurring in the southern segment of the Goiás Magmatic Arc, in the Neoproterozoic Brasilia Belt. The intrusions are broadly associated with the Brazilian Orogeny and have been interpreted as syntectonic intrusions associated with the second magmatic event in the Arennópolis Arc, but the specifics of the origin and emplacement of these mafic bodies are poorly constrained (Augustin and Della Giustina, 2019; Laux et al., 2004; Mota-e-Silva et al., 2011; Nilson and Santos, 1982). In this paper, we present new field and petrographic descriptions, lithogeochemistry of the cumulate rocks, and the results of thermodynamic modeling aimed at better understanding the characteristics of the parental magma of the complex.

## 2. Regional and local geology

The Goiás Magmatic Arc (Fuck et al., 1994; Pimentel and Fuck, 1992) is a Neoproterozoic tectonic unit located in the westernmost Brasília Belt (Fig. 1), which is one of the three large Neoproterozoic orogens that resulted from the collisions of the Amazonian, São Francisco-Congo and Paranapanema cratons and smaller allochthonous blocks (Fig. 1A). The Goias Magmatic Arc trends NE-SW and its northern and southern limits are covered by the Parnaiba and Parana Basins, respectively (Fig. 1B). It comprises two domains separated by the Goiás Archean Block (e.g. Pimentel, 2016). The northern domain is known as the Mara Rosa arc and the southern is called the Arenópolis arc (Pimentel et al., 2000). Both branches show geological, geochemical, and geochronological similarities, which suggests they probably shared a common evolution (Laux et al., 2005, 2004; Matteini et al., 2010; Pimentel et al., 2004). The igneous activity in the Goiás Magmatic Arc occurred in two main episodes: a first magmatic stage between ca. 890 and 800 Ma, characterized by the eruption of primitive tholeiitic to calc-alkaline volcanic rocks and intrusion of associated tonalites and granodiorites formed in an island arc setting, and a second magmatic stage, dated around 670–600 Ma, in which calc-alkaline magmatism was accompanied by metamorphism and deformation in an active convergent continental margin (Fuck et al., 2017; Laux et al., 2005, 2004; Matteini et al., 2010; Pimentel, 2016; Pimentel et al., 2004; Pimentel and Fuck, 1992).

The Arenópolis arc comprises N—S trending volcano-sedimentary sequences (e.g. Bom Jardim de Goiás, Arenópolis, Iporá, Jaupaci, and Anicuns-Itaberaí, respectively from west to east), separated from each other by calcic- to calc-alkaline diorite to granite orthogneisses (Fuck et al., 2017). The supracrustal and orthogneiss units of the Arenópolis arc are juxtaposed along regional NNE to NNW strike-slip fault systems, which are part of the continental-scale Transbrasiliano Lineament (Pimentel et al., 2000). The eastern portion of the Arenópolis Arc is limited by the granulite-facies gneisses of the Anápolis-Itauçu Complex (Baldwin et al., 2005; Piuzana et al., 2003).

The mafic–ultramafic intrusions of the Arenópolis arc were first recognized during an undergraduate geologic mapping exercise conducted by the Institute of Geosciences of the University of Brasilia in 1969 (Danni et al., 1973). Two mafic–ultramafic bodies were mapped, the Mangabal Massif – currently called Mangabal Complex (Augustin & Della Giustina, 2019) – and the São João Massif – currently known as the Americano do Brasil Complex (hereafter ABC; Danni et al., 1973; Nilson, 1981; Mota-e-Silva et al., 2011; Fig. 1C).

Nilson (1981) first described the ABC as a small layered pluton consisting of mafic and ultramafic cumulate rocks containing ubiquitous megacrysts of poikilitic pargasitic hornblende, with associated amphibolite facies minerals. The ABC was emplaced into orthogneisses and minor mica-schist of the southern domain of the Goiás Magmatic Arc. The complex became well known due to the development of the Americano do Brasil underground Ni-Cu-Co mine developed through a

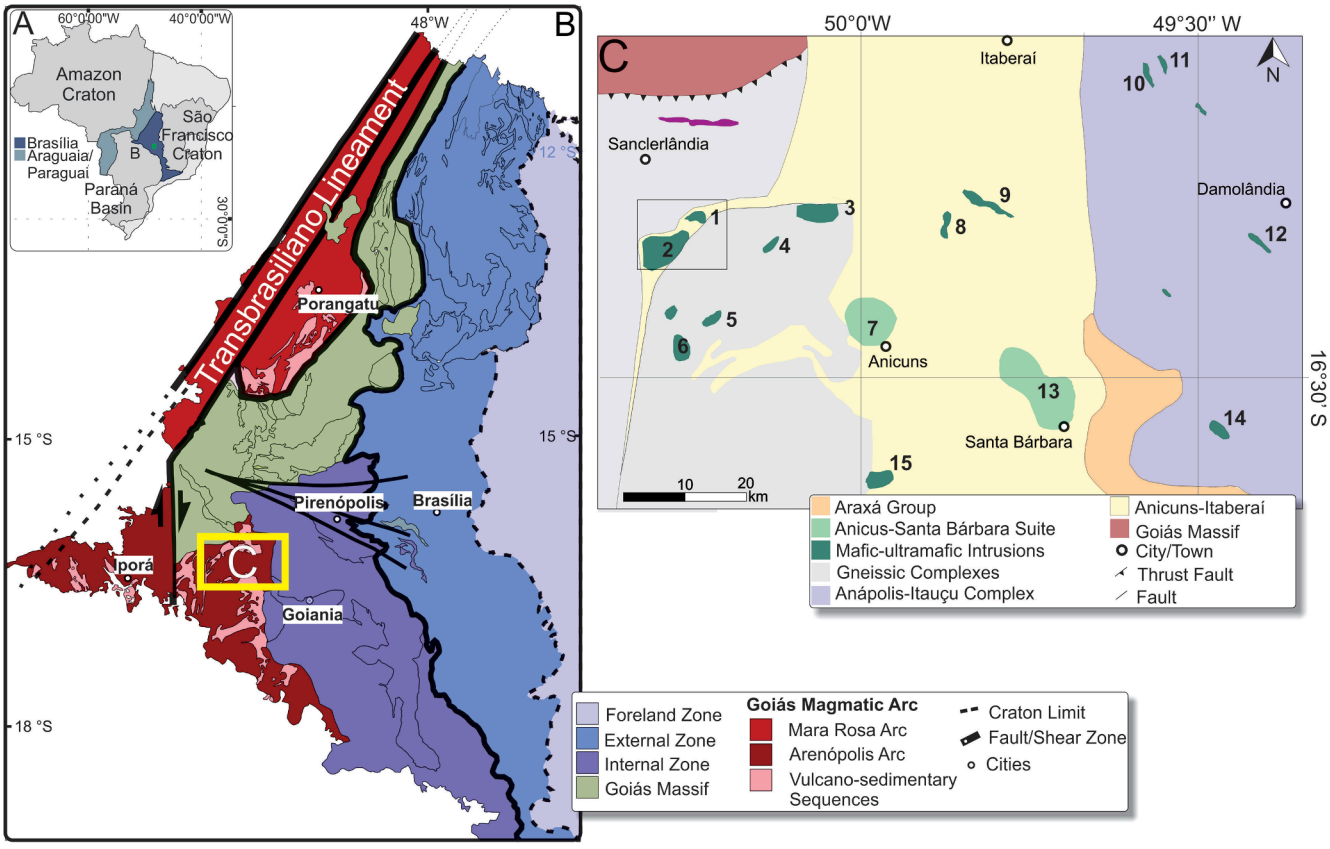


**Fig. 1.** A) Spatial location of Brasilia Belt in Brazil. B) Brasilia Belt schematic geological map (modified after Pimentel et al., 2004; Macedo et al., 2018, colours differentiate tectonic zonations. Goiás Magmatic Arc in dark red. C) Simplified geological map of the area indicated in B.

joint venture between Prometalica Ltd. and Votorantim Metais Ltd., which ended operations in 2014. It was the object of geological survey and mineral exploration, including drilling and some petrographic studies of cumulate rocks and associated Ni-Cu sulfide ore (Mota-e-Silva et al., 2011; Nilson, 1981, 1984; Nilson and Santos, 1982). In the most recent work, the ABC has been interpreted as two distinct E–W-trending mafic–ultramafic sequences juxtaposed along the Salgado fault (Mota-e-Silva et al., 2011). Regional isotopic studies indicated positive $\varepsilon_{Nd}$ (+3.1) and a TIMS U-Pb zircon age of 626 ± 26 M, obtained from two zircons separated from a sample described as olivine-pyroxene norite (Laux, 2004; Nilson et al., 1997).

## 3. Analytical methods

### 3.1. Sample collection

Samples from four representative drill cores (numbers AMB317, AMB366, AMB443, and AMB427) were selected for sampling based on the core-logging at the mine. The rock samples were selected to represent the different lithological associations and the stratigraphy of the complex. Polished thin sections were examined under transmitted/reflected polarizing microscopes to ensure the identification of all major rock types as well as their mineral associations and crystallization sequences, textures, and superimposed recrystallization due to metamorphism and deformation.

### 3.2. Whole-rock major and trace elements

Twenty-five sample powders from the Americano do Brasil Complex and two internal standards (samples 18-CR-14-1 and 18-CR-14-2) were analyzed at ALS geochemistry laboratories using a package for a complete sample characterization (ALS code CCP-PKG01). Whole-rock major elements ($SiO_2$, $Al_2O_3$, $Fe_2O_3$, CaO, MgO, $Na_2O$, $K_2O$, $Cr_2O_3$, $TiO_2$, MnO, $P_2O_5$, SrO, BaO) were analyzed via Inductively Coupled Plasma Atomic Emission Spectrometry (ICP-AES) on samples prepared by the lithium borate fusion method followed by nitric acid digestion (ME-ICP06). Base metals (Ag, Cd, Co, Cu, Mo, Ni, Pb, Sc, and Zn) were digested in four acids (perchloric, nitric, hydrofluoric and hydrochloric acids), and then their concentrations were also determined by ICP-AES (ME-4ACD81). Trace lithophile elements were analyzed by Inductively Coupled Plasma–Mass Spectrometry (ICP–MS) after the same lithium borate fusion and digestion as for the major oxides method (ME-MS81). The concentrations of As, Bi, Hg, In, Re, Sb, Se, Te and Tl were analyzed by ICP-MS after digestion in aqua-regia (ME-MS42). Total sulfur and carbon were analyzed by LECO infrared spectroscopy (ME-IR08). Platinum, palladium and gold were determined by standard lead bead collection fire assay and ICP-MS finish. The geochemical data are given in the Supplementary file. To permit comparison of samples that experienced different degrees of alteration, geochemical data used in this work were normalized to a volatile-free basis.

### 3.3. Mineral chemistry

The compositions of major rock-forming minerals from several polished thin sections were determined by electron probe microanalysis (EPMA). Analyses were performed using a JEOL JXA-8230 SuperProbe with five wavelength dispersive spectrometers (WDS) at the University of Brasilia. Operating conditions for all silicate minerals were 15 kV accelerating voltage, a beam current of 10nA and probe diameters of 1 μm for all minerals except plagioclase (5 μm). Counting times on peak and background were 10 s and 5 s, respectively. Energy dispersive X-ray spectroscopy (EDS) of several minerals was also performed to support petrographic studies.

## 4. Geology of Americano do Brasil Complex

The area around the Americano do Brasil Complex is dominated by pasture and intense weathering, which can reach up to 40 m depth locally. The exposures are mostly small loose blocks and the best preserved occurrences are associated with amphibole-bearing rocks. Due to the lack of spatially extensive outcrops, drill cores were important to improve the understanding of the complex and its rocks.

In general, the ABC is about 2.5 km in length and about 1.5 km in width and is divided into two sequences by the E-W oriented Salgado Fault (Fig. 2). It is dominated by ultramafic cumulates; to the north of the fault, the most common rocks are olivine and olivine-pyroxene-cumulates, whereas the Southern portion has more evolved compositions dominated by pyroxene and pyroxene-plagioclase cumulates. Primary igneous textures are dominant, but a metamorphic overprint is marked by fracturing and sub-grain fragmentation due to dynamic recrystallization, twinning deformation, corona reactions, recrystallization and partial to complete replacement of the primary mineralogy by a hydrous assemblage (e.g. amphiboles, serpentine, chlorite). Intense amphibolitization is ubiquitous in the complex. Pegmatitic diorite and minor dolerite (-to gabbro) dykes commonly crosscut the complex, but they are more prominent and voluminous in the Southern portion.

### 4.1. Rock types of the Americano do Brasil Complex

Although deformed and partially recrystallized, the ABC still preserves some relict igneous features, which we emphasize in this work. Distinct primary rock types are distinguished on the basis of texture and mineralogical composition and will be here described according to the location related to the E-W fault (e.g. Northern and Southern sequences). The amphibolite-facies assemblage and metamorphic rocks will only be described when important for better clarification.

The rocks of the Complex range from adcumulate to heteradcumulate texture, and the nomenclature is based on the recognizable cumulus minerals, even though some rocks contain sufficient postcumulus material to be compositionally classified in another way. The cumulate term is used in this work to describe the texture of the rock and does not imply any specific mechanism for the formation of the cumulus minerals.

#### 4.1.1. Northern sequence

The Northern sequence is dominated by olivine adcumulates, i.e., dunite, that gradually transition to lenses and/or layers of olivine-clinopyroxene adcumulate, i.e., wehrlite.

Olivine cumulate is a massive medium-grained rock, ranging in colour from black, when fresh, to yellowish-grey when weathered. It contains abundant subhedral to anhedral olivine, commonly occurring as subrounded and equidimensional to slightly elongated crystals. Cumulus Cr-spinel occurs as inclusions in olivine and in the matrix, its amount does not exceed 2 % of the volume of the rock. The texture is most commonly adcumulate with up to 5 % intercumulus pyroxene and amphibole, but it locally shows a mesocumulate texture. Olivine is commonly altered to serpentine and magnetite in a mesh texture (Fig. 3A), secondary chlorite, carbonate, and talc are also common alteration products in these rocks.

The olivine-clinopyroxene adcumulate (or clinopyroxene-olivine cumulate) occurs as layers or lenses, showing gradational contacts with enclosing packages of dunite in the south, and increases in volume to the north. In hand-specimen the rock is grayish, due to the appearance of clinopyroxene as cumulus mineral. It is a medium- to coarse-grained cumulate, which consists of rounded to sub-rounded olivine and subhedral clinopyroxene grains (Fig. 3B); the former is commonly altered to serpentine in a mesh texture and the latter into amphibole (tremolite to magnesium hornblende). Minor (<1 vol%) cumulus chromium-rich magnetite occurs either as inclusions or interstitial to cumulus olivine and pyroxene. Subordinate orthopyroxene occurs locally as distinct

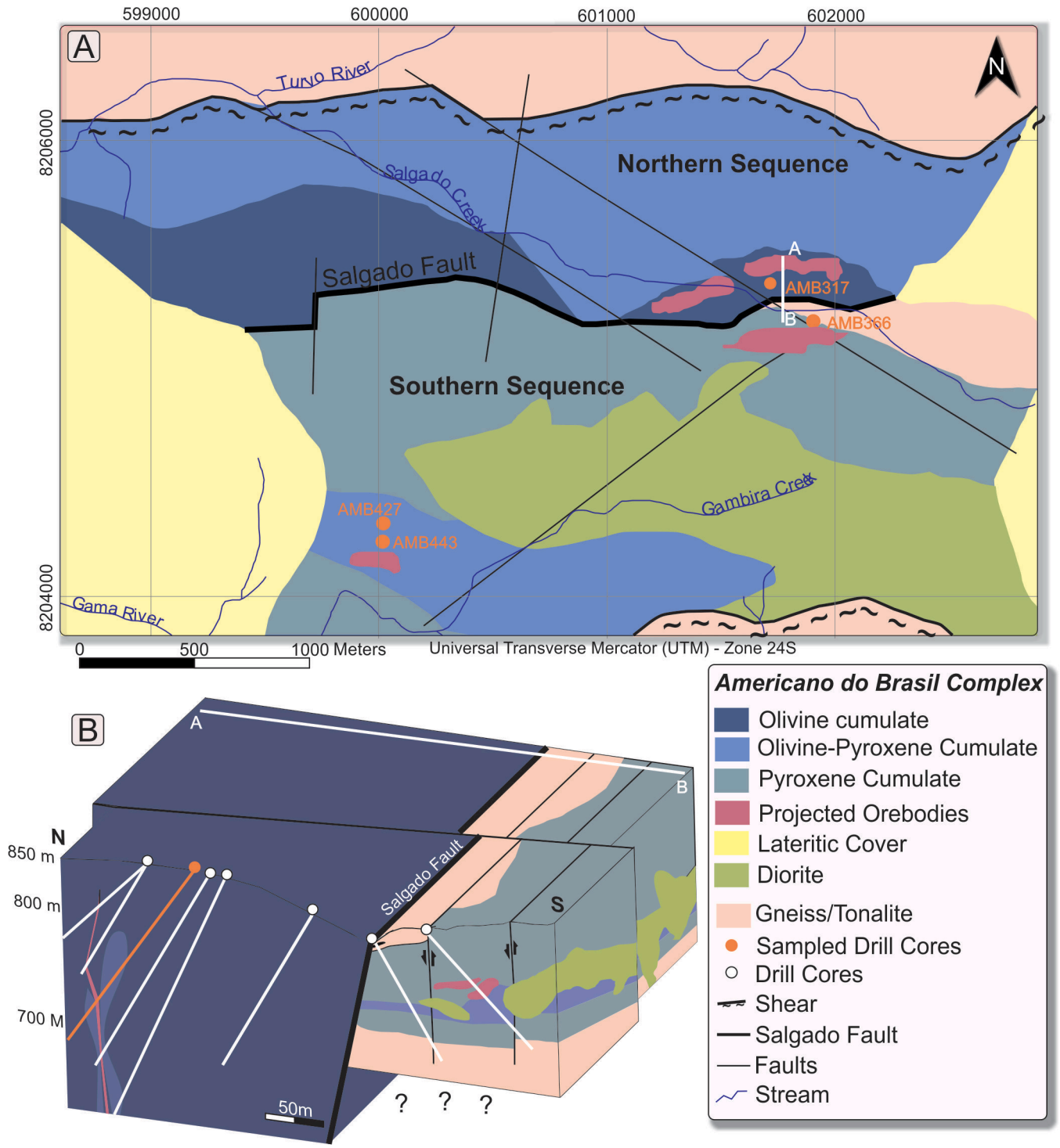


**Fig. 2.** A) Geological map of the Americano do Brasil Complex adapted after Nilson (1981) and Mota-e-Silva et al. (2011). B) Schematic cross section of the A-B line (drawn in 1.A) showing the simplified relationship of the southern and northern sequences along the Salgado's fault.

equant cumulus grains rather than as oikocrysts, generally not exceeding 5 % of the cumulus portion. Some isolated portions of the rock contain higher amounts of interstitial amphibole (up to 10 %), typically with a dusty appearance resulting from needle-like exsolution of iron–titanium oxides. Locally, it is possible to identify the replacement of the borders of olivine by granoblastic orthopyroxene (Fig. 3C) and/or orthopyroxene-magnetite symplectites in corona textures.

#### 4.1.2. Southern sequence

To the south of the Salgado fault, the rocks of the ABC are rich in pyroxenes, plagioclase and/or hornblende. The primary mineralogy is widely transformed into secondary hydrous minerals due to superimposed regional metamorphism and/or hydrothermal alteration spatially associated with dioritic dykes. The Southern sequence has a more intense amphibolitization compared to the Northern sequence and more voluminous dioritic veins.

The most common rock in this portion is clinopyroxene-

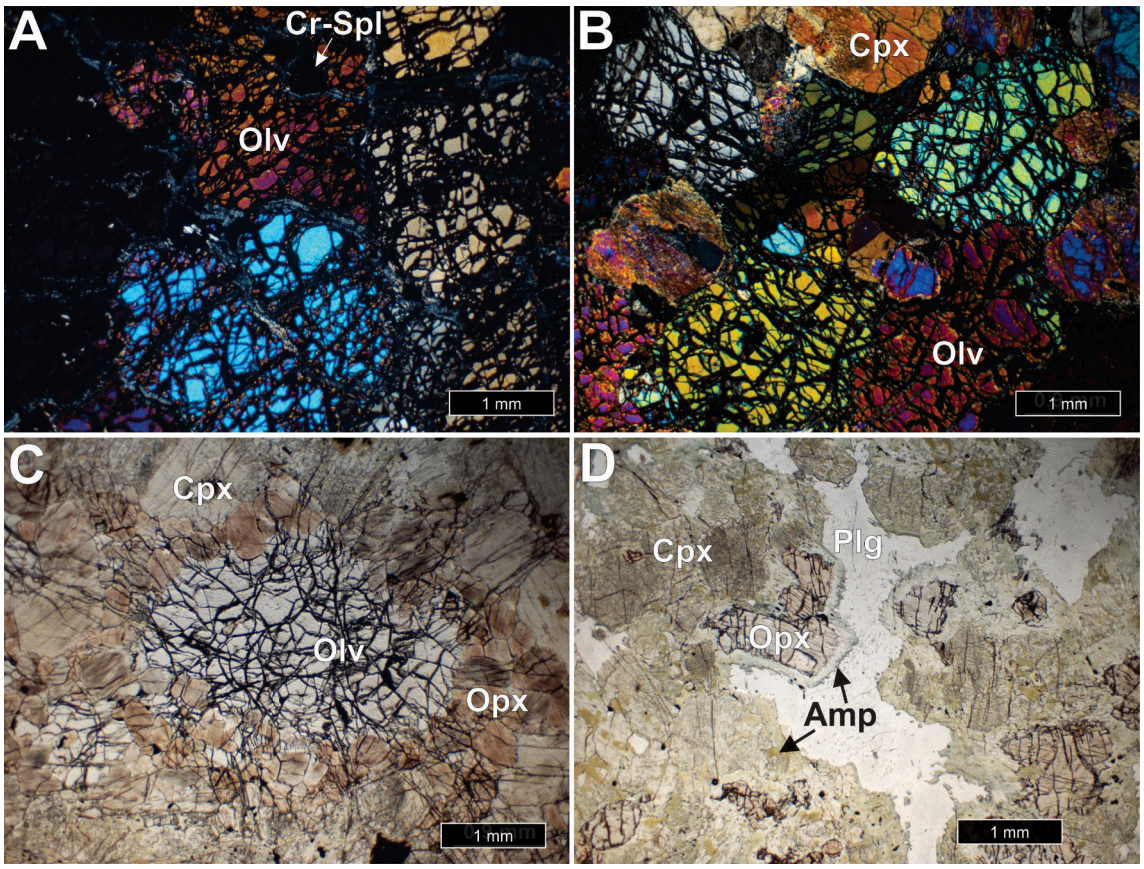


**Fig. 3.** Photomicrographs of cumulate rocks of the Americano do Brasil Complex. (A) Olivine cumulate in cross-polarized light. (B) Olivine-clinopyroxene cumulate in cross-polarized light. The clinopyroxene is partially replaced by amphibole and olivine by serpentine in mesh texture. (C) Detail in plane-polarized light of clinopyroxene-olivine cumulate, with granular orthopyroxene corona around olivine. (D) Pyroxene-cumulate in plane-polarized light; clinopyroxene is intensely replaced by amphibole with needle-like exsolutions of Fe-Ti oxides. Pyroxene-plagioclase contact is almost completely mantled by an amphibole corona.

orthopyroxene cumulate, ranging locally to pyroxene-plagioclase cumulate. In places, thick packages of these rocks have their original texture and mineralogy completely overprinted by metamorphic assemblages, and here are described as metaultramafics.

Two-pyroxene cumulate is medium-grained, with approximately equal amounts of cumulus clinopyroxene and orthopyroxene that range from subhedral to euhedral. Clinopyroxene crystals commonly show substitution by secondary hornblende along crystallographically controlled planes and rims, locally small preserved relict clinopyroxene grains remaining in the core. Orthopyroxene is generally rimmed by secondary amphibole when in contact with plagioclase (Fig. 3D), similar to clinopyroxene. Plagioclase and minor hornblende are the most common interstitial minerals; the latter can occur as poikiloblasts, encompassing the relict orthopyroxene crystals. The modal proportion of cumulus and intercumulus grains is difficult to define due to intense reaction of pyroxenes and plagioclase with metamorphic hydrous fluids to form amphiboles. This transformation is mainly spatially associated with the diorite veins. In addition to pyroxene, a smaller amount of cumulus olivine or plagioclase appears locally. Olivine, when present, is partial to almost completely replaced by orthopyroxene in corona textures and/or replaced by symplectites of iron oxides and orthopyroxene. Sulfides and oxides occur as interstitial material between pyroxene and are commonly included in the other interstitial minerals such as plagioclase. The pyroxene-plagioclase cumulate is found locally as layers/lenses. It is textured similarly to the two-pyroxenexe cumulate rocks, marked by the appearance of small amounts of cumulus plagioclase.

The southwestern portion of the ABC contains some olivine-pyroxene cumulates, which are associated with massive to semi-massive sulfides. These are composed of olivine, clinopyroxene and orthopyroxene, the latter occurring as minor cumulus grains and more voluminous oikocrysts encompassing olivine. The silicates occur mainly as clasts in a sulfide-matrix breccia. In sulfide-poor portions, interstitial amphibole (pargasite) occurs in poikilitic texture and commonly replaces clinopyroxene oikocrysts almost completely. The textural relations between the primary cumulus phases are obscure due to the lack of preserved primary contact and pervasive recrystallization of the igneous minerals.

#### *4.1.3. Sulfide mineralization*

The sulfide mineralization in Americano do Brasil forms 3 orebodies, one of them, named S2, located within the Northern sequence, and the other two, known as G2 and S1, appearing in the Southern sequence.

The S2 orebody is composed of cumulus olivine, partially serpentinized to a mesh-texture, enclosed in a net-textured to semi-massive sulfide matrix (Fig. 4A). The intercumulus sulfide consists of pyrrhotite, chalcopyrite, and pentlandite, in descending order of abundance. Pyrrhotite exhibits minor exsolved flames of pentlandite. Pentlandite also occurs as polycrystalline aggregates along with pyrrhotite crystals, mainly close to serpentine-filled fractures and commonly in contact with olivine. Chalcopyrite occurs in anhedral aggregates. Pyrite is secondary and occurs filling fractures and/or parting planes of sulfides, commonly associated with serpentine veins. Extensive serpentinization has visible effects on the sulfides, which are highly fractured. Serpentine and magnetite veins crosscut the primary sulfides. The sulfides cut by veins associated with hydrous alteration are commonly replaced by secondary minerals along the fractures, where magnetite replaces pyrrhotite and cubanite is formed after chalcopyrite.

In the northeastern portion of the Southern sequence, the S1

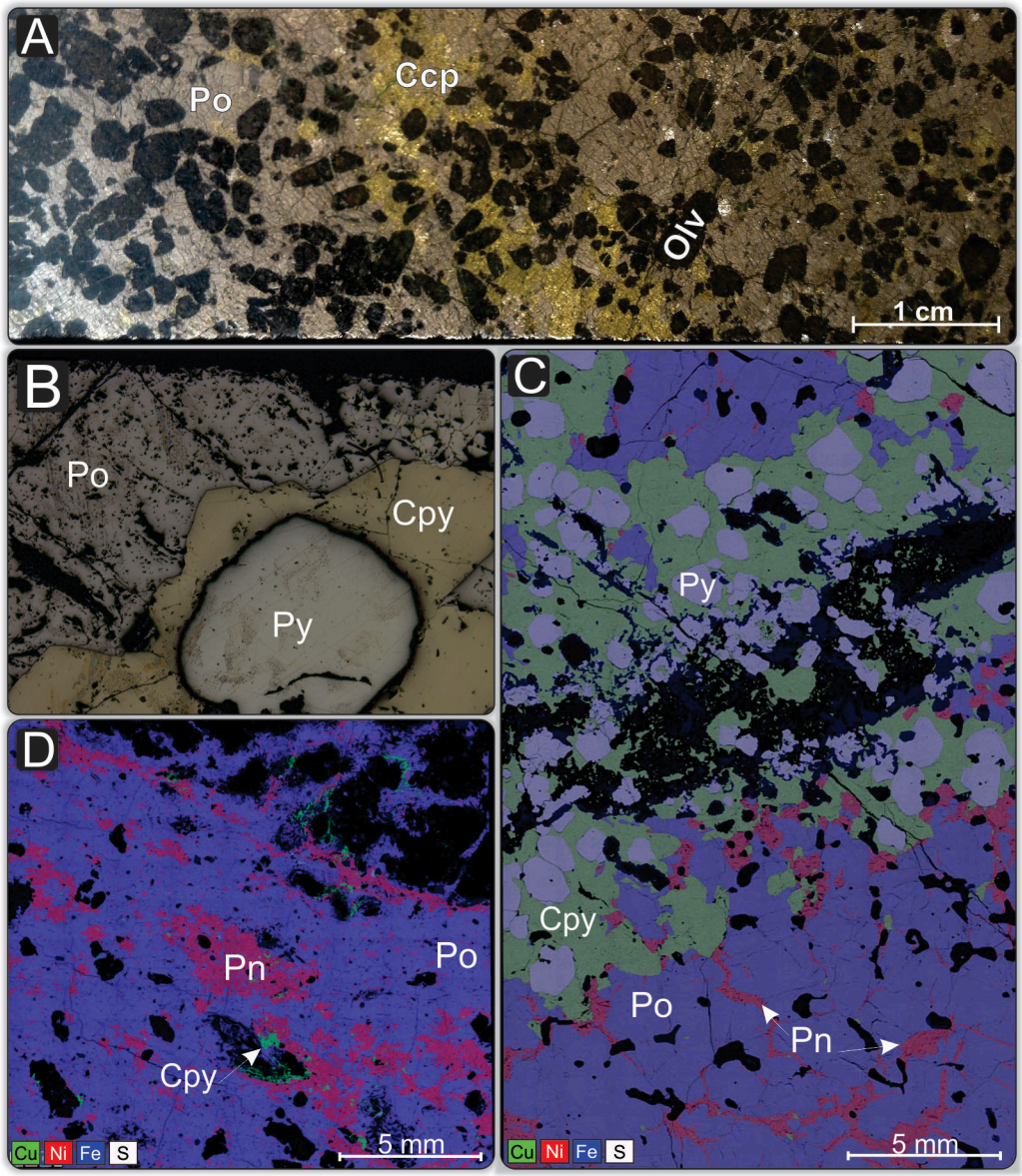


**Fig. 4.** (A) Semi-massive ore in olivine cumulate, sample from S2 orebody. (B) Reflected light photomicrograph of the thin section containing core of pyrite, sorrunded by rim of chalcopyrite in pyrrhotite matrix. (C) C-D) Compositional EDS maps. (C) Massive sulfide sample from the S1 orebody showing close relationship of pyrite-chalcopyrite-magnetite assemblage with hydrous-rich vein crosscutting the section. (D) Massive ore from G2 orebody with tectonically mobilized and recrystallized massive ore, showing granoblastic textures and foliation defined by flattened pentlandite aggregates.

orebody, which ranges from disseminated to lenses of massive sulfide, is mainly hosted by pyroxene cumulates and pyroxene-plagioclase cumulates. The sulfides are composed of pyrrhotite with associated pentlandite, chalcopyrite, and pyrite. The S1 orebody includes portions with typical magmatic textures such as large blebby pyrrhotite and pentlandite exsolution (loops or flames can occur) and minor chalcopyrite. The pyrite is commonly surrounded by chalcopyrite rims and immersed in the pyrrhotite matrix, with zoning visible on a macroscopic as well as at microscopic scales (Fig. 4B). Pyrite-rich domains are commonly associated with hydrothermal veins rich in carbonates and/or silicates, such as quartz, biotite, amphibole. Anhydrite is also found associated with alteration zones. The sulfides closely associated with hydrous minerals/veins are altered from a pyrrhotite-pentlandite-chalcopyrite association into pyrite-chalcopyrite, with magnetite locally occurring close to silicate phases (Fig. 4C).

The G2 orebody occurs in the southwestern portion of the Southern sequence and is hosted by olivine-pyroxene cumulates. The ore textures range from net-textured to massive breccia, with localized tectonic *durchbewegung* (german for "through motion or movement", defined by Ramdohr, 1960) *breccias*. The massive ore comprises a matrix of sulfide with floating or imbricated inclusions of the ultramafic clasts and/or minerals, with phenocrysts commonly replaced by sulfides. The sulfide mineralization has the typical magmatic sulfide assemblage of pyrrhotite, pentlandite and chalcopyrite, but is intensely recrystallized, evidenced by granoblastic textures and foliation defined by flattened pentlandite aggregates (Fig. 4D). Portions richer in phyllosilicates such as serpentine can show preferred strong planar alignment and folding, concordant with exsolved pentlandite in pyrrhotite. In these foliated portions, silicate inclusions are strongly replaced by hydrous phases including serpentine, amphiboles and talc. Some inclusions of silicate minerals were replaced by pseudomorphs of sulfide.

#### 4.1.4. *Country rocks and later intrusions*

The complex was emplaced into the tonalitic gneiss of the Turvânia block (Fig. 1B), which is commonly composed of a thinly banded and foliated rock dominated by plagioclase, hornblende, quartz, biotite and epidote, with minor K-feldspar, chlorite, garnet and titanite. At the northernmost exposures, garnetiferous mica schist crops out, concordant with the foliation of the gneisses. All the observed contacts of the ABC complex with the gneissic rocks are tectonic and marked by shear zones, in which gneisses are mylonitized and altered to an assemblage of sericite, epidote and carbonate.

The dioritic veins can be varitextured, showing variations from fine to very coarse-grained over short distances. They are more commonly pegmatoidal, consisting basically of equal amounts of euhedral hornblende, reaching up to 4 cm in length, and plagioclase, which is commonly white due to intense saussuritization. The veins vary from millimeters to meters in thickness and occur in more than one generation. The rocks in contact with and close to the veins show intense amphibolitization, reaching locally up to 80 % of amphibole. These amphibole-dominant rocks adjacent to diorite were described in previous works as hornblendites, metapyroxenites and/or pyroxenites.

Dolerite occurs as dykes that range from 1 cm to up 5 m in thickness that crosscut the complex, the gneissic host rocks and the dioritic veins. It is commonly recrystallized to granoblastic assemblages of clinopyroxene, plagioclase, orthopyroxene, ilmenite, and magnetite. It is very fine grained, with a relict porphyritic texture, where it is possible to identify former plagioclase phenocrysts that have undergone dynamic recrystallization. Fe-Ti oxides are abundant, occurring both as relict phenocrysts and in the matrix. Sulfide minerals, including pyrite, chalcopyrite, and pyrrhotite, are present in trace amounts. In the interiors of larger dolerite dikes (~5 m), the grain size increases to a medium-grained but still non-cumulate (diabasic-textured) gabbro. Where the dolerite has undergone local deformation, it is completely transformed into a very fine grained foliated rock with an amphibolite assemblage marked by hornblende, plagioclase, oxides and apatite.

## 5. Geochemistry

### 5.1. Mineral chemistry

Although the olivine is largely replaced by serpentine, it is still possible to identify relict grains preserved well enough to permit quantitative analysis on the EPMA. Analyzed olivine in the Americano do Brasil Complex ranges from $Fo_{80}$ to $Fo_{87}$ (Fig. 5A). In the Northern sequence, the forsterite content (Fo) ranges from 80 to 84, while Ni content varies from 1300 to 2950 ppm. In the Southern sequence, olivine was identified only in the G2 orebody, where it has compositions ranging from $Fo_{85}$ to $Fo_{87}$, and Ni content ranging from 479 to 1524 ppm. In a plot of Ni in olivine versus Fo content (Fig. 5A), the Ni concentrations in olivine increase slightly with increasing Fo in the Northern sequence; the Southern sequence has a lower Ni content.

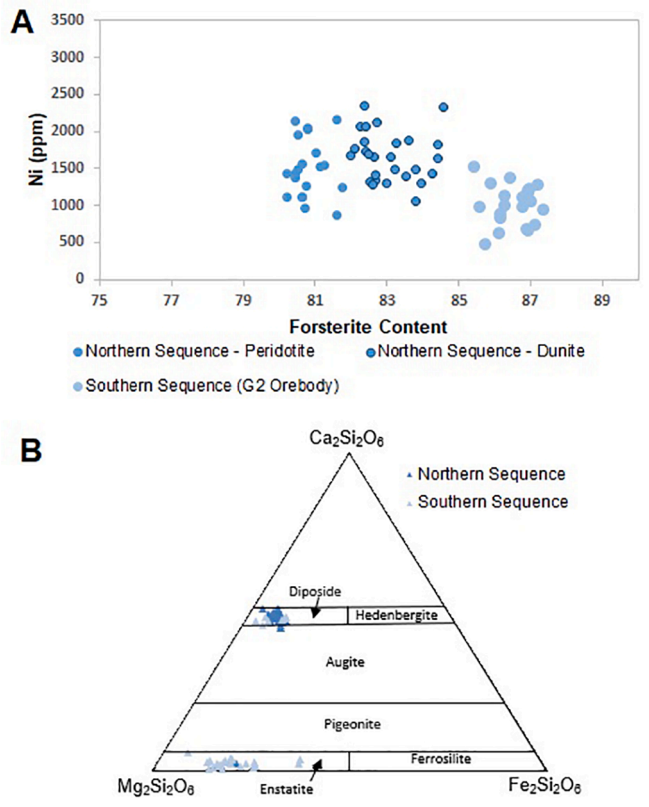


**Fig. 5.** A: Plot of forsterite content vs Ni (ppm) in analyzed olivine. B: Orthopyroxene and clinopyroxene compositions for cumulate minerals. Pyroxene nomenclature is from (Morimoto, 1988).

Clinopyroxene in both sequences is diopside with a few compositions straddling the augite-diopside boundary (Fig. 5B). Clinopyroxene from the Southern sequence of Americano do Brasil contains up to 0.5 wt% $TiO_2$, $Al_2O_3$ up to 3.4, $Cr_2O_3$ reaching up to 0.3, and magnesium-number (molar 100*Mg/Mg + Fe; Mg#) ranging from 70 to 88. Clinopyroxene from the Northern sequence is similar with values of up to 0.68 wt% $TiO_2$, 4.7 wt% $Al_2O_3$, 0.83 wt% $Cr_2O_3$ and Mg# between 78 and 93. Orthopyroxene is classified as enstatite with compositions ranging between $En_{81}$ and $En_{84}$ in the Northern sequence and from $En_{74\text{-}84}$ in the Southern sequence.

### 5.2. Major element geochemistry

Whole-rock compositions of the different lithologies analyzed in this study are given in Supplementary Table 1. The concentration of the major elements in rocks of the Americano do Brasil Complex is inferred to be mainly controlled largely by variation in the proportions of the cumulus minerals (olivine and/or clinopyroxene), but the quantity of intercumulus material has some influence, mainly in the Southern sequence, where the textures are more variable compared to the Northern sequence and there is more interstitial plagioclase. Rocks from the Northern Sequence analyzed in this study have MgO content that ranges from 42 to 24 wt%. There are well-defined trends of negative correlation of $SiO_2$, $Al_2O_3$, CaO and $Na_2O$ with MgO (Fig. 6), as a result of the removal of mafic minerals from a liquid. The FeO has a positive correlation with MgO.

Although the pyroxene cumulates of the Southern portion show similar trends (Fig. 7), these are not as well defined, due to highly variable modal proportions of cumulus phases and intercumulus material, which reach up to 40 vol% in volume. In rocks of the Southern sequence, the MgO concentrations are much lower, ranging from 12.4 wt% to 18.4 wt% while the FeO content ranges from 12.7 to 14.9 wt%. The $Al_2O3$ and $Na_2O$ contents show well-defined trends due to the presence of plagioclase, ranging from 8 to 15.5 wt% and up to 0.5 wt% respectively. The CaO concentration is variable, ranging from 7.3 up to 13.1 wt%, where the highest values occur in rocks richer in clinopyroxene than orthopyroxene.

The diabasic rocks (and related gabbros) have characteristics of more evolved rocks. They have lower values of MgO ranging from 5 to 8 wt%, and values of $Na_2O$ and $Al_2O_3$ ranging up to almost 5 wt% and 21 wt% respectively. Overall, the diabase has much more evolved compositions than the rocks of the complex, with distinct lower MgO content, and higher $Na_2O$ and $Al_2O_3$, showing a separate cluster from the measured rocks of the complex.

### 5.3. Trace element geochemistry

Primitive mantle-normalized rare-earth element (REE) and incompatible trace-element patterns of rocks from Americano do Brasil are shown in Fig. 8. In general, the rocks from the southern sequence have higher values in REE and trace elements. Olivine-clinopyroxene and clinopyroxene-orthopyroxene cumulates are enriched in middle REE (MREE) relative to both light REE (LREE) ($La_N/Sm_N = 0.1$ to 0.5 and 0.7 – 0.9 in the Northern and Southern respectively) and heavy REE (HREE) ($Sm_N/Yb_N = 1.6$–3.1 and 1.6–2.2 in the Northern and southern respectively). The Northern sequence shows a deeper HREE depletion compared to the Southern sequence ($Gb_N/Yb_N = 1.7$ to 4.0 in the Northern sequence, and 1.2 to 1.8 in the Southern sequence). The olivine

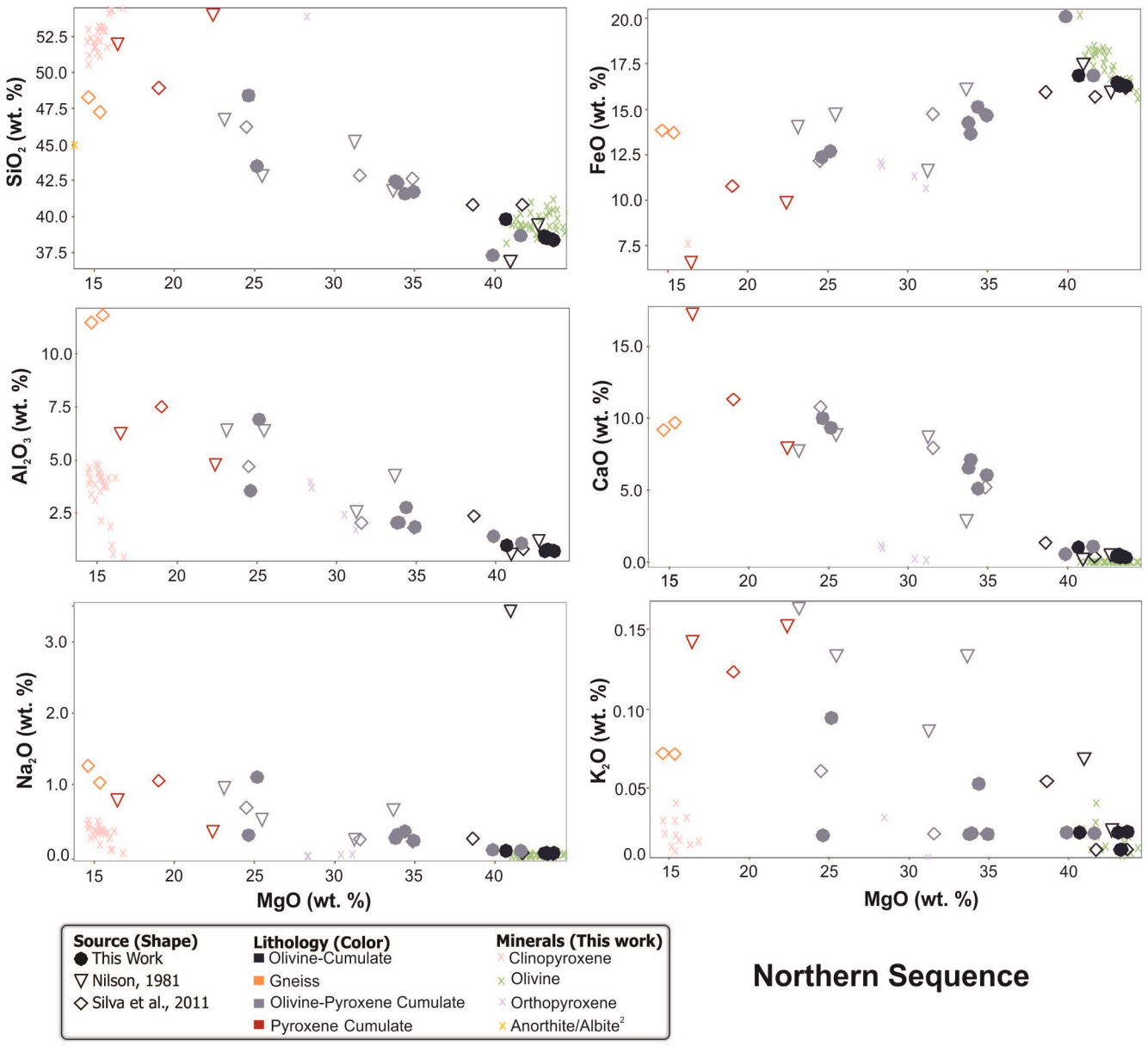


**Fig. 6.** Whole-rock $SiO_2$, FeO, $Al_2O_3$, CaO, $Na_2O$ and $K_2O$ vs MgO bivariate plots for Northern sequence.Filled circles are from this work, outlined triangle and diamond shapes are from Mota-e-Silva et al. (2011) and Nilson (1981) respectively. Olivine (OLV), clinopyroxene (CPX) and orthopyroxene (OPX) were values measured in this work. DU olivine cumulate, PD olivine-pyroxene cumulate, PX pyroxene cumulate, GT pyroxene-plagioclase cumulate, GN gneiss.

cumulate from the Northern sequence and the diabase rocks from the Southern sequence are enriched in LREE relative to HREE, without the MREE enrichment in clinopyroxene cumulates.

Most of the rocks show some similarities in the patterns in the multi-element diagram. The samples are not enriched in large-ion lithophile elements (LILE) relative to high-field strength elements (HFSE) in general, but some of them (Th, U and Ta) are below or close to their lower limits of quantificatio006E. A distinctive positive Sr anomaly is ubiquitous, and negative Zr, Hf, P, and Nb anomalies are identified in all rocks of the Southern sequence.

## 6. Discussion

### 6.1. Thermodynamic modeling

In order to address the composition and evolution of the melt parental to the cumulates of both the Northern and Southern portions of the Americano do Brasil Complex, we have modeled crystallization using the alphaMELTS thermodynamic software (Asimow, 1998; Ghiorso and Sack, 1995; Smith and Asimow, 2005). The contacts of the complex with the country rocks are marked by intense shearing and/or metamorphic/hydrothermal alteration, preventing the preservation and identification of a chilled margin. Also, no volcanic rocks or dikes have been identified that could be inferred to be compositional equivalents to the initial liquid. Several basaltic compositions representing mafic rocks/liquids described elsewhere along the extent of the Brasília Belt (e.g. Girardi et al., 1986; Laux et al., 2010; Correia et al., 2012; Brown et al., 2020; Piauilino et al., 2021) were tentatively used to estimate the composition of the initial liquid, but the mafic volcanic rocks described so far do not have Mg# high enough to form the most magnesian olivine of the Complex, nor would they generate similar cumulus assemblages in general.

In an effort to find a reasonable starting liquid composition for modeling the evolution of the suite, a wide variety of other known

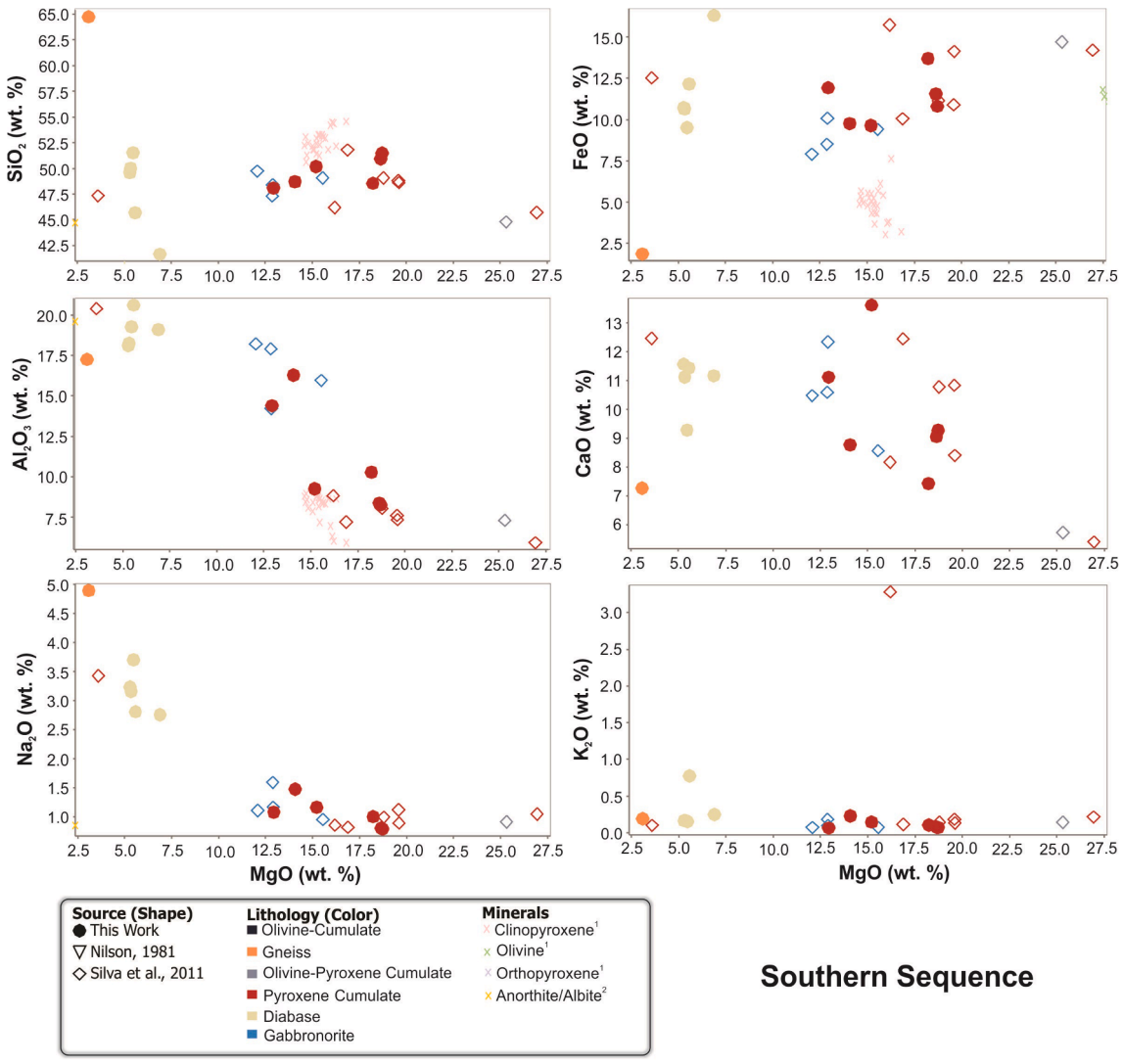


**Fig. 7.** Whole-rock $SiO_2$, FeO, $A_{l2}O_3$, CaO, $Na_2O$ and $K_2O$ vs MgO bivariate plots for Southern sequence. Filled circles are from this work, outlined triangle and diamond shapes are from Data from Mota-e-Silva et al. (2011) and Nilson (1981) respectively.. Olivine, clinopyroxene, orthopyroxene and plagioclase were values measured in this work (X symbol). The colours are the same from Fig. 5. PX pyroxene cumulate, GT pyroxene-plagioclase cumulate, GN gneiss. DB diabase.

primitive basaltic liquid compositions were considered, all of which have been proposed as the parental magmas to other known layered intrusions around the world, e.g. Penchenga, Jinchuan, Duke Island, Georgia Arc picrites (Chai and Naldrett, 1992; Li and Ripley, 2011; Naldrett, 2004; Ramsay et al., 1984; Thakurta et al., 2008). All petrological simulations were done using various pressures between 1.0 and 7.5 kbar, $H_2O$ contents ranging from 0.5 % to 4 % and oxygen fugacities $fO_2$ between −1.5 and + 1.5 log units relative to FMQ (fayalite–magnetite–quartz solid oxygen buffer). However, the thermodynamic modeling results from all of these hypothetical parental magmas were inconsistent with the observed mineral assemblages and chemical compositions of the natural rocks.

We eventually settled on the composition of a picrite from the Mid-Continent Rift (of the Keweenawan large igneous province) in Minnesota, USA (Lightfoot et al, 1999), which we selected because it combines a relatively Fe-rich character with moderate LILE and HFSE enrichment, similar to the patterns observed in the ABC, and is of broadly similar Proterozoic age in agreement with the Goiás Magmatic Arc ages. Comparison of the composition of this parental liquid and the ultramafic cumulates of the Northern Sequence of the Americano do Brasil complex suggests that the Northern sequence formed from a magma very similar to the Mid-Continent Rift magma, with little to no evidence of contamination by its country rocks nor any other persuasive indication of a crustal signature.

Efforts to reproduce the observed cumulate compositions using a model of their accumulation from the parental liquid during a process of fractional crystallization were unsuccessful for two reasons. First, due to the peritectic reaction between olivine and orthopyroxene, concomitant precipitation of olivine and pyroxene was not achieved in any fractional crystallization models. In contrast, in an equilibrium crystallization model, olivine and orthopyroxene coexist over a wide range of temperatures and modal proportions. Second, there is no evidence of a systematic decrease in whole-rock Mg#, forsterite content of olivine, or decreasing anorthite content of plagioclase with stratigraphic position consistent with fractional removal of forsteritic olivine and anorthitic plagioclase.

Thus, the working hypothesis was that it might be possible to produce representatives of each cumulate via batch crystallization from a primitive liquid. Nilson (1981) estimated that the pressure of emplacement for the Americano do Brasil Complex was up to 5 kbar. Using the empirical model described by Putirka (2008), the clinopyroxene-orthopyroxene pairs in cumulates of the Northern Sequence indicate ranges of 2–5 kbar, with $K_D(Fe\text{-}Mg)^{cpx\text{-}opx}$ ranging from 0.7 to 0.8, which lies around the indicated parameters for subsolidus equilibration. Thus,

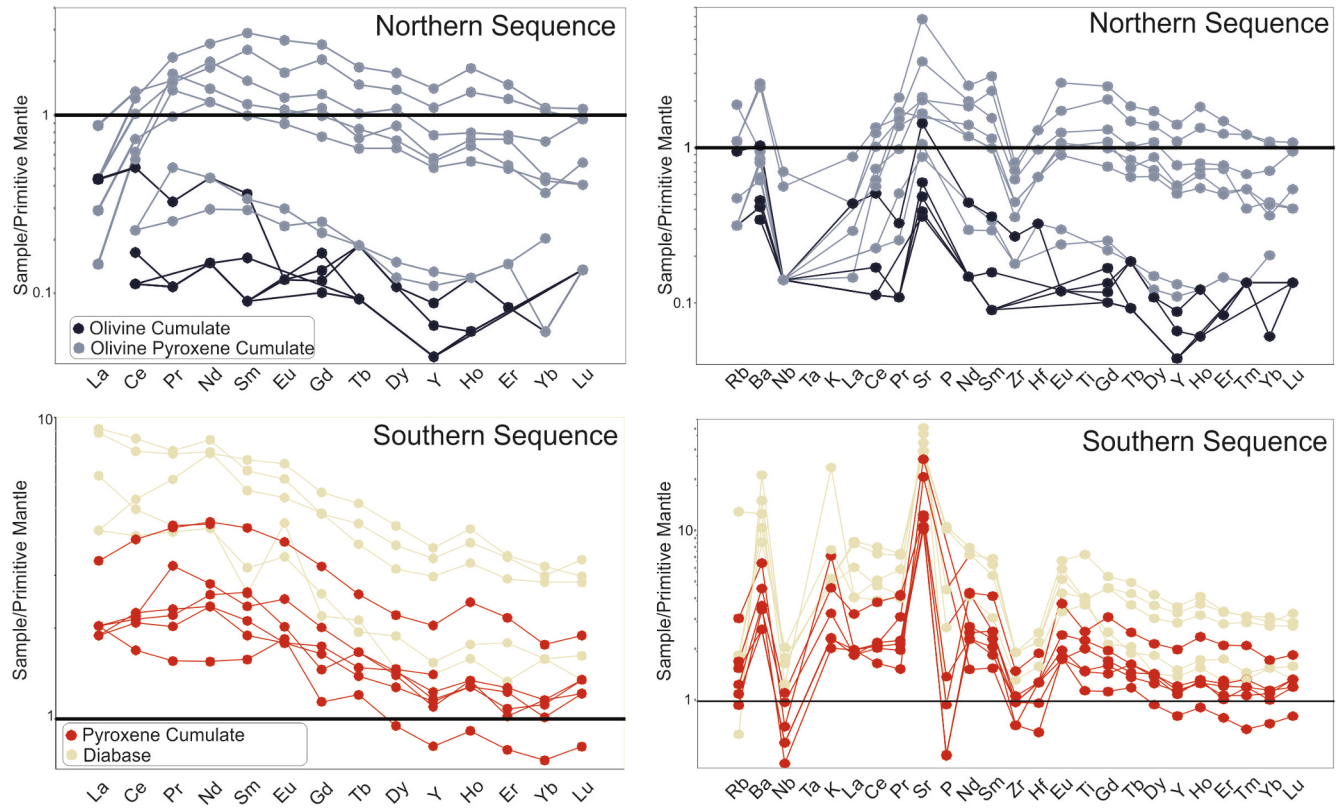


**Fig. 8.** Primitive mantle normalized REE and multi-diagram trace element patterns for both northern and southern sequences of Americano do Brasil Complex. Normalization from Sun and Mcdonough (1989).

we considered a pressure consistent with previous geological constraints and also the amphibolite facies assemblage presently observed. Cooling of our chosen picrite under isobaric conditions at 2.5 kbar and $fO_2$ 0.5 log units above the FMQ produced a similar sequence of crystallization and modal proportions of solids to the observed bulk-rock and mineral compositions of all major constituents of the Northern sequence of Americano do Brasil. This model predicts the crystallization of olivine ($Fo_{88}$) starting at a liquidus temperature of 1310 °C, followed by the appearance of clinopyroxene (Mg# 82) at 1190 °C and orthopyroxene (Mg#81) at 1170 °C. Between 1220 °C and 1150 °C the model predicts the entire range of ultramafic rocks analyzed in the Northern sequence. Modeled olivine, clinopyroxene and orthopyroxene compositions show good agreement with much of what is measured in the rocks ($Fo_{83\text{-}79}$, $En_{82\text{-}80}$, $En_{80}$, respectively), as well as the whole-rock major element concentrations. A comparison of modeled solids and natural occurrences is shown in Table 1. The range of compositions of olivine and pyroxene could be entirely accounted for by a model of batch crystallization of the picrite liquid, followed by accumulation of crystals in slightly different proportions, and subsequent re-equilibration of minerals and up to 5 % trapped liquid during cooling, consistent with the adcumulate texture. The REE distribution pattern of the measured samples and model is comparable in Fig. 9. The success of the batch crystallization model implies that the cumulates were emplaced into the complex as batches or slurries of crystals that remained entrained in the magma during varying degrees of cooling.

The Southern sequence is represented mainly by pyroxene cumulates and minor pyroxene-plagioclase cumulates. Rocks similar to the ones in this sequence can be predicted by modeling the same picrite combined with the assimilation of country rock in an isenthalpic process following an assimilation batch crystallization process. We use similar conditions to the Northern Sequence, at 2.5 kbar and $fO_2$ + 0.5 log units above the FMQ. A granodioritic country rock from Americano do Brasil Complex, at an initial temperature of 300 °C, was assimilated in 1 g increments into 100 g of the picrite (beginning at a temperature of 1310 °C) under isenthalpic conditions at a constant pressure of 2.5 kbar and $fO2$ 0.5 log units above the FMQ. During a process of between 22 and 45 % assimilation of granodiorite, the system cools to 1120 °C and crystallizes solids similar to the rocks analyzed in the Southern sequence. The modeled rocks range from orthopyroxene-clinopyroxene cumulates to gabbro, with different modal proportions of the main minerals. To

**Table 1**
Results of MELTS model compared with rocks of the Americano do Brasil Complex. Picrite liquid used is sample #7 from Lightfoot et al. (1999).

| **Sequence** | **Northern** | | | | | |
|---|---|---|---|---|---|---|
| **Conditions:** | 2.5 Kbar, FMQ + 0.5, H2O 0.5 % | | | | | |
| | Olivine Cumulate | | Olivine-Clinopyroxene Cumulate | | Olivine-Clinopyroxene-Orthopyroxene Cumulate | |
| | Model | Natural | Model | Natural | Model | Natural |
| **Liquidus (°C)** | 1220–1200 | – | 1180–1190 | – | 1170–1190 | – |
| **Mineralogy** | Olivine, Cr-spinel | Olivine, Cr-spinel | Olivine, Cr-spinel, Clinopyroxene | Olivine, Cr-spinel, Clinopyroxene | Olivine, Cr-spinel, Clinopyroxene, Orthopyroxene | Olivine, Cr-spinel, Clinopyroxene, Orthopyroxene |
| **Fo** | 83 | 82–83 | 80–81 | 80–82 | 77–79 | 80–81 |
| **mg# (Cpx)** | – | – | 82 | 78–87 | 81–80 | 83–84 |
| **mg#(Opx)** | – | – | – | – | 80–81 | 78–82 |

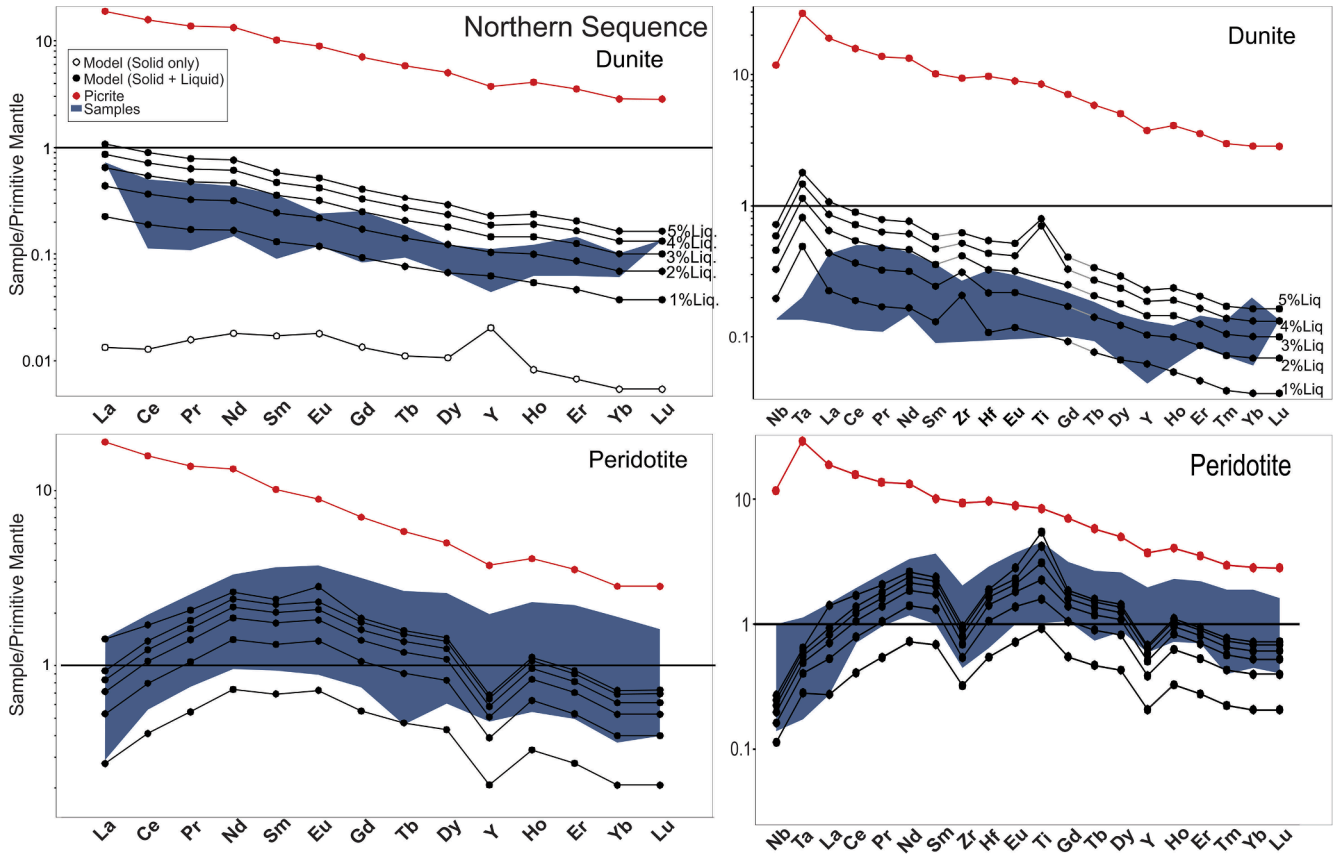


**Fig. 9.** Primitive mantle-normalized REE and multi-element plots for natural and model rocks from the Northern sequence of the ABC. The shaded portion shows the range of compositions of rocks of Americano do Brasil Complex. Normalization from Sun and Mcdonough (1989). The black lines represent modeled cumulate rocks with indicated weight fractions of trapped liquid and red is the picrite magma used as the parental liquid in the models (#7, Lightfoot et al., 1999).

match the overall abundance of incompatible trace elements in the bulk cumulate rocks, model cumulates require the presence of up to 15 wt% trapped liquid with the solids. Because there are different degrees of contamination, the ranges of compositions of the rocks vary. The trace-element abundances of the cumulates ranging from the least evolved pyroxene cumulate to the most evolved gabbro and their modeled equivalents are shown in Fig. 10. The model results are given in Supplementary Table 2.

### 6.2. *Mantle source and parental magma*

In order to have a better understanding of the tectonic setting and conditions of formation of the Americano do Brasil Complex, it is important to constrain the nature of the mantle source and crystallization order of the parental magma of the rocks. The petrographic analyses show that the crystallization order for the intrusions was olivine-clinopyroxene-orthopyroxene-plagioclase for the Northern sequence and olivine-orthopyroxene-clinopyroxene-plagioclase for the Southern sequence. The crystallization order differs partially from the previous

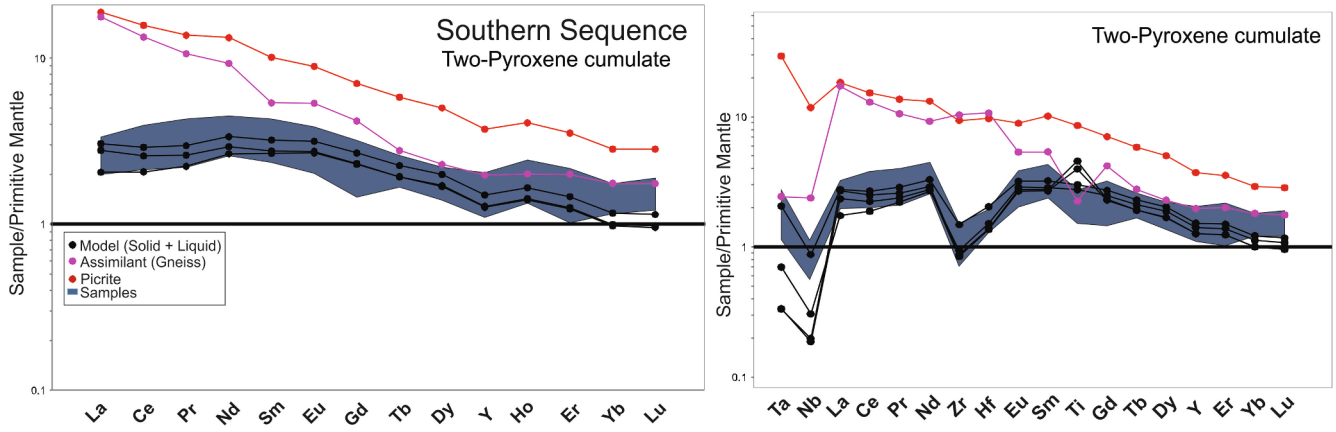


**Fig. 10.** Primitive mantle-normalized REE and multi-element plots for rocks from the Southern sequence of the ABC compared with model results. Normalization from Sun and Mcdonough (1989). The blue polygon covers the range of few compositions of rocks of Americano do Brasil Complex samples. The black lines represent modeled cumulate rocks with trapped liquid, red is the picrite used as initial liquid (#7, Lightfoot et al., 1999), and pink is the composition of the assimilant gneiss.

works. Mota-e-Silva et al., (2011) described the same order of crystallization for both sequences, with orthopyroxene preceding clinopyroxene; whereas Nilson (1981) did not subdivide the complex into two sequences and concluded from the textures that clinopyroxene crystallized prior to orthopyroxene in the Northern sequence. Therefore, our results are partially in agreement with both works, showing that indeed there are slight differences in the crystallization orders of the two sequences. The highest forsterite content in olivine from Americano do Brasil measured in this study was $Fo_{87}$. The well-known olivine-melt distribution coefficient ($K_D$: 0.3; Roeder and Emslie, 1970) indicates that the liquid in equilibrium with the most primitive olivine grains had an Mg/Fe ratio of 2.3, which indicates that the parental liquid for the earliest olivine cumulates had similar Mg/Fe (ratio) as the picritic liquid used in the modeling.

The clinopyroxene-cumulate rocks of both sequences are enriched in MREE relative to both LREE and HREE (Fig. 8). The two sequences have previously been interpreted to have crystallized from a similar parental magma due to a similar crystallization trend and both being enriched in MREE relative to LREE and HREE (Mota-e-Silva et al., 2011). The REE and trace element patterns for rocks from both sequences documented here have some similar patterns and are accounted for well by the thermodynamic modeling described above, which shows that rocks from both sequences could be formed from the same parental liquid, which evolved along distinctly different paths under different conditions such as degrees of contamination, indicating that the intrusions are potentially comagmatic and could represent different portions of the same system.

The significance of the enrichment in MREE relative to LREE and HREE was previously assigned as a characteristic inherited from the parental liquid and was used to infer a depleted-mantle source to the liquid due to the LREE depletion (Mota-e-Silva et al., 2011). In contrast to this idea, our modeling indicates that the LREE depletion relative to MREE can be attributed to accumulation of clinopyroxene, which shows this pattern due to the variation of partition coefficients along the lanthanide series. The presence of abundant MREE-enriched clinopyroxene also explains the higher LREE depletion compared to MREE in olivine-clinopyroxene adcumulates than in the two-pyroxene-cumulates, which we infer to have contained more trapped liquid. The HREE depletion relative to LREE and MREE, on the other hand, is not related to specific cumulate minerals and is probably a signature of the parental magma. Although the model parental liquid may have a slightly stronger relative depletion in HREE than the real parental magma for the complex, the Americano do Brasil Complex still has moderate HREE fractionation indicating the parental magma probably had at least moderate fractionation in heavy rare earth elements too, which may require residual garnet in a deep source or a contribution from pyroxenitic mantle. The picrite liquid used in our model is more similar to an ocean-island basalt (OIB) than to a normal-type mid-ocean ridge basalt (*N*-MORB) (Lightfoot et al., 1999; Shirey et al., 1994), but displaced to lower concentrations than typical OIB. The lower overall trace element concentrations are consistent with its picritic composition as compared to the basaltic compositions used to define typical OIB signatures. We use the close match of our modeled cumulate compositions to the natural compositions to infer that the parental magma of the Americano do Brasil complex was an OIB-like Fe-rich picrite, and that all of the rocks of both the northern and Southern portions of the complex were likely to have shared this common parent. Despite the similarities in patterns, the Southern sequence has higher concentration of REE and trace elements when compared to the Northern sequence. The difference is explained by the assimilation of the country rock as well as the influence of trapped liquid, as shown by the modeling. We do not intend to correlate the ABC directly with the MCR picrite; rather, we used it only to infer the chemical characteristics of the ABC parental magma and suggest that a liquid with a similar composition and age could have formed by similar asthenospheric processes to generate the rocks of the complex.

### 6.3. Constraint from sulfide chemistry

The equation described by Campbell and Naldrett (1979) is used to calculate the distribution of metal between silicate melt and an immiscible sulfide liquid, for a given mass ratio $R$ of silicate liquid to sulfide liquid in a closed system. The $R$-factor equation is $X_{sulf} = X_0 \times \frac{D(R+1)}{R+D}$, where $X_{sulf}$ is the concentration of the element in the sulfide melt, $X_o$ is the concentration of the element in the initial silicate melt, and $D$ is the partition coefficient defined as the concentration in the sulfide phase divided by the concentration in the silicate melt at equilibrium. However, post-magmatic processes such as metamorphism and deformation may influence the distribution and morphology of the ore, which is evident by the presence of durchbewegung texture in massive sulfide, serpentinization in net-textured sulfide and the presence of pyrite in some zones associated with hydrous secondary mineral assemblages. Fig. 11 shows the sulfide metal tenors for the mineralization in the ABC and the closed-system $R$-factor model curves for the parental picrite liquid used in the modeling and for the liquid remaining after 45 % of assimilation. The measured sulfide compositions fall at R values between 100 and 10,000 and are bracketed by the model curves for sulfide segregation from melts ranging from the parental picrite to the most strongly contaminated magma we have modeled.

There is a wide range of ore tenors between the various ABC ore bodies and, to the extent that compositions have not changed during metamorphism, it could imply an inhomogeneous system with wide local variations in effective $R$-factor. The metal content of the S1 orebody has a broad variation, ranging from values similar to the other orebodies (S2 and G2) to very low Ni and Cu content when compared to sulfide abundance. Overall, the S1 body appears to result from sulfide saturation later in the evolution of the magma than does S2 or G2. Also, the $R$ factor required to model some samples in the S1 orebody shows a wide variation and does not follow a single path for equilibration with the magmatic liquids inferred to have been present based on the thermodynamic modeling above. The failure of a simple model of primary $R$-factor control of sulfide tenor for some samples implies that some post-emplacement changes in the system may have promoted S or metal mobilization. The post-magmatic events, such as deformation and interaction with hydrothermal fluids, may have locally overprinted some of the primary magmatic textures, resulting in localized sulfide mobilization and the variations of Ni/Cu ratio between sulfide samples. The relative roles of primary $R$ factor control versus post-magmatic alteration will be approached in a further study focused in post-magmatic overprints.

### 6.4. Emplacement constraints

The intrusion does not show much evidence for exclusively fractional crystallization from a single pulse of magma. Neither the forsterite content nor the enstatite content of pyroxenes show a clear fractionation trend according to stratigraphic height, nor are there very well defined layers. Our observations and model results indicate that the evolution of the magmatic system by fractional crystallization, as classically understood, would not have produced the observed sequence of rock types. In particular, the occurrence of olivine-orthopyroxene cumulates is forbidden by the peritectic relationship between these two phases. On the other hand, there is a wide range of conditions under which olivine and orthopyroxene can coexist during batch crystallization, with or without the concurrent process of host rock assimilation.

In order to enable batch crystallization, a system with a hot and low viscosity magma is required for the crystals to be able to re-equilibrate continuously, a situation favored by turbulent flow and/or vigorous forced convection to keep the crystals suspended while they react with the melt (e.g., Barnes et al., 1995; Yao et al., 2021). Assimilation-batch crystallization processes, as applied in this work, have been used to model the evolution of magmas that fed large mafic–ultramafic

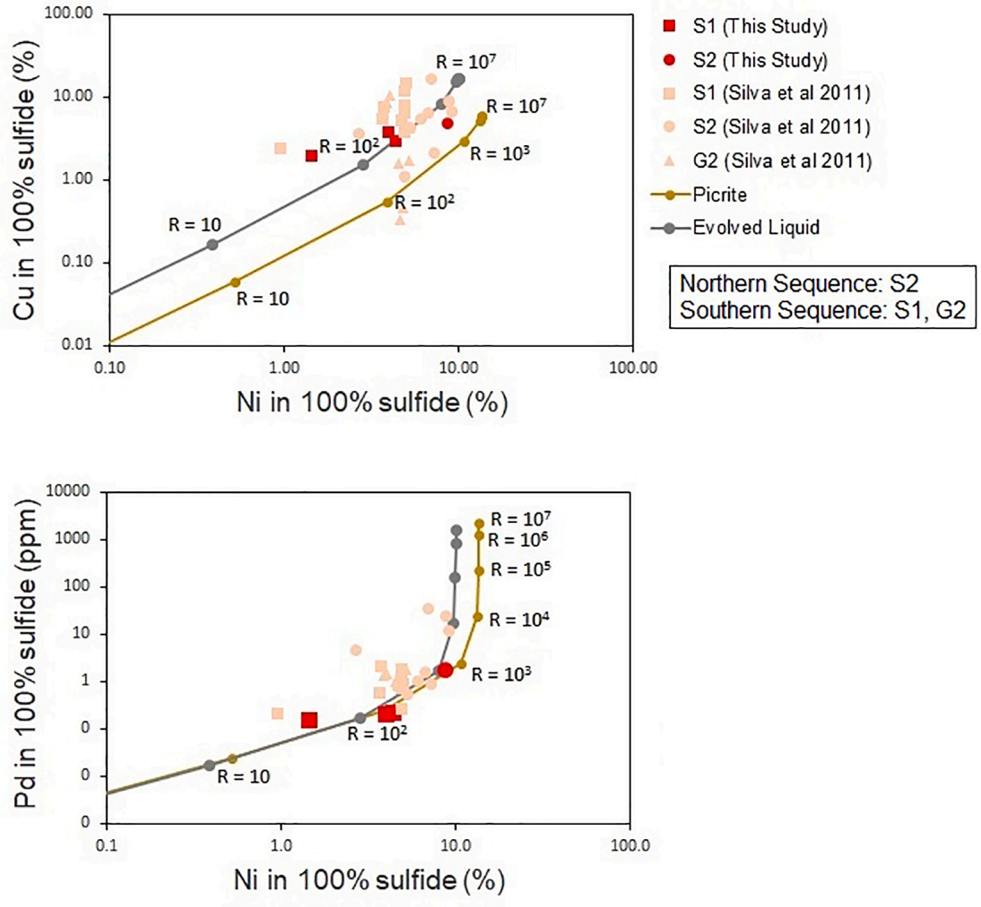


**Fig. 11.** Bivariate plot showing the calculated sulfide metal tenors for individual samples for the three orebodies of Americano do Brasil (S1, S2 and G2) compared to Picrite used in model and the most evolved liquid modeled for pyroxene-cumulates after assimilation. Red are data acquired in this study, pink are from Silva et al. (2011). Calculated base metal sulfide tenors (Cu in 100 % sulfide vs Ni in 100 % sulfide). *R*-factor model curves were calculated using the closed-system *R*-factor model (Campbell and Naldrett, 1979). The model picrite had a bulk composition with 59 ppm Cu, 540 ppm Ni, and 2.5 ppb Pd. The partition coefficients (*D*) between the sulfide and basaltic liquids were 1,000, 250, and 1,000,000 for Cu, Ni, and Pd, respectively. The evolved liquid had a bulk composition of 168 ppm Cu, 400 ppm Ni, and 1.7 ppb Pd.

intrusions such as the Bushveld and Stillwater complexes, but also can be applied to smaller and irregular-shaped intrusions like Americano do Brasil (e.g., Barnes et al., 1995; Jenkins et al., 2021; Jenkins and Mungall, 2018; Yao et al., 2021). In addition, previous works focused on modeling and field relations have shown that picrite and komatiites can assimilate high amounts of crustal rocks because the heat generated by the fusion of the assimilant is compensated by the heat of crystallization of the cumulates (e.g., Mungall, 2007). As shown by these previous studies and our present modeling results, the picrite liquid used in the present study is capable of large degrees of host rock assimilation due to its high temperature and steeply descending liquidus slope.

Several geologic criteria for defining magma conduit systems were previously described (Li et al., 2001; Maier et al., 2011, 2001) such as a high proportion of sulfides, presence of associated volcanic rocks overlying the intrusion, tube shape and evidence for multiple phases of intrusion. Unfortunately, the record of metamorphism, tectonism and erosion, in addition to poor exposure and hence few constraints on the shape of the intrusion, makes it difficult to grasp the details of the geometry of the ABC or link it to some conduit system or related lava flows. However, the rocks of the Complex are dominated by cumulates, and like those described in many other magmatic Ni-Cu-PGE (e.g., Barnes et al., 1995; Lesher, 1989)must be lacking some residual liquid complement. The country rocks have been previously interpreted as representing rocks of the island arc stage of the Brasilia Belt (Laux et al., 2004) and the area of study is related to the younger deep crustal Magmatic Arc (Laux et al., 2004); however, the pressure of crystallization of the Complex appears to have been typical of the upper to middle crust and there is no petrographic or geochemical evidence for high-pressure crystallization as would be expected in the roots of a continental magmatic arc. We suggest that the intrusion could have been emplaced in the middle or upper crust due to ascent in locally extensional weak zones, possibly in a sill-like conduit system.

### 6.5. *Element mobility and post-cumulus modification*

Post-magmatic processes, such as metamorphism or weathering, may result in considerable changes to the original geochemistry of the rocks. The degree of alteration in the ABC can be noted in high loss on ignition (LOI) of the rocks, which ranges from below 0.5 to up to 13 %, with the highest values associated with intensely serpentinized olivine cumulates. The intrusion has been affected by amphibolite-facies metamorphism (Nilson, 1981), and has zones showing intense alteration to amphiboles and the apparent input of hydrothermal/metamorphic fluid, evidenced by increased abundance of secondary pyrite associated with these alteration zones. This pervasive alteration is associated with the percolation of fluids close to shear zones, with the notable presence of anhydrite, carbonate- and/or amphibole in veins linked to cross-cutting diorite dikes and associated alteration. Abundances of fluid-mobile elements such as Ba, K and Sr show different patterns than predicted from geochemical modeling; but because they are highly mobile elements, these mismatches could directly be attributed to fluid-mediated metasomatism during the regional metamorphism.

A variety of plots based on comparison of trace elements ratios to igneous suites of well-understood provenance are commonly used as indicators of petrogenetic affinity (e.g. La/Sm, Ba/Yb, Nb/Ce). However, there are several reasons why most of them cannot be used to discuss the lithogeochemical signature of the Americano do Brasil Complex. Firstly, most of them are constructed based on liquid compositions, which made the cumulates rocks not suitable for application (e.g. Pearce et al., 2021). Elements that can be compatible with the

cumulus minerals in these rocks cannot be meaningfully compared with highly incompatible elements that could represent the trapped liquid, because this would have no petrogenetic significance. Elements prone to fluid transfer also cannot be used reliably to classify rocks that have been subjected to extensive metamorphic overprints.

On the other hand, the diabasic-textured doleritic rocks follow similar major and trace element geochemical trends as the pyroxene cumulates of the Southern sequence, but cross-cutting relations with both the cumulate rocks of the Southern sequence of the complex and the dioritic-veins suggest a younger age for the diorites.

## 7. Conclusions

The Americano do Brasil Complex is composed of ultramafic to mafic cumulates and has been affected by metamorphism to the amphibolite facies, resulting in intense amphibolitization and recrystallization. Much of the intrusion maintains its primary magmatic textural features because deformation and hydrothermal alteration tend to have been restricted to discrete shear zones, veins and/or the margins of the intrusion. Post-magmatic processes such as metamorphism or deformation may have influenced the distribution and morphology of the mineralization.

Modeling indicates that the parental magma of the intrusion had an OIB-like Fe-rich picrite composition and that the same primary liquid could be parental to rocks from both the Northern and Southern sequences. The differences between the Northern and Southern sequences resulted from different degrees of crustal assimilation, within different portions of the same magmatic system. The intrusion formed by equilibrium crystallization with different proportions of assimilation, emplaced at a mid- to upper-crustal level, at pressure around 2.5 kbar, and melt temperatures as high as 1310 °C. The depletion in HREE indicates a deep source with some residual garnet, and the MREE enrichment in some rocks is associated with the accumulation of clinopyroxene instead of being a signature of the parental magma.

## Declaration of Competing Interest

The authors declare that they have no known competing financial interests or personal relationships that could have appeared to influence the work reported in this paper.

## Data availability

Data will be made available on request.

## Acknowledgments

CTA thanks Antonio Peixoto from Prometalica Mineração Centro-Oeste S/A for providing access to samples. This paper is part of the Ph.D. work of C.T.A. This study was financed in part by the Coordenação de Aperfeiçoamento de Pessoal de Nível Superior – Brasil (CAPES) – Finance Code 001 and Fundação de Apoio a Pesquisa do Distrito Federal (FAP/DF - project number 800/2019). This research has been partly supported by Canadian NSERC grant CRDPJ 523131-17, and this is publication number 88 of the Large Igneous Provinces -Industry Consortium Project (www.supercontinent.org). Comments by reviewers and editors led to considerable improvement in the paper.

## Appendix A. Supplementary data

Supplementary data to this article can be found online at https://doi.org/10.1016/j.oregeorev.2022.105126.

## References

Asimow, P.D., 1998. Algorithmic modifications extending MELTS to calculate subsolidus phase relations. Am. Mineral. 83, 1127–1132. https://doi.org/10.2138/am-1998-9-1022.

Augustin, C.T., Della Giustina, M.E.S., 2019. Geology and metamorphism of the neoproterozoic Mangabal Complex: An example of Ni–Cu-PGE mineralized intrusion in the Goiás Magmatic Arc, central Brazil. J. South Am. Earth Sci. 90, 504–519. https://doi.org/10.1016/j.jsames.2018.12.013.

Baldwin, J.A., Powell, R., Brown, M., Moraes, R., Fuck, R.A., 2005. Modelling of mineral equilibria in ultrahigh-temperature metamorphic rocks from the Anápolis-Itauçu Complex, central Brazil. J. Metamorph. Geol. 23, 511–531. https://doi.org/10.1111/j.1525-1314.2005.00591.x.

Barnes, S.J., Lesher, C.M., Keays, R.R., 1995. Geochemistry of mineralised and barren komatiites from the Perseverance nickel deposit, Western Australia. Lithos 34, 209–234. https://doi.org/10.1016/0024-4937(95)90023-3.

Barnes, S.J., Osborne, G.A., Cook, D., Barnes, L., Maier, W.D., Godel, B., 2011. The Santa Rita nickel sulfide deposit in the Fazenda Mirabela Intrusion, Bahia, Brazil: Geology, sulfide geochemistry, and genesis. Econ. Geol. 106, 1083–1110. https://doi.org/10.2113/econgeo.106.7.1083.

Barnes, S.J., Mole, D.R., Hornsey, R., Schoneveld, L.E., 2019. Nickel-copper sulfide mineralization in the ntaka hill ultramafic complex, Nachingwea Region. Tanzania Econ. Geol. 114, 1135–1158. https://doi.org/10.5382/econgeo.4677.

Brown, M.T., Fuck, R.A., Dantas, E.L., 2020. Isotopic age constraints and geochemical results of disseminated ophiolitic assemblage from Neoproterozoic mélange, central Brazil. Precambrian Res. 339, 105581 https://doi.org/10.1016/j.precamres.2019.105581.

Campbell, I.H., Naldrett, A.J., 1979. The influence of silicate:sulfide ratios on the geochemistry of magmatic sulfides. Econ. Geol. 74, 1503–1506. https://doi.org/10.2113/gsecongeo.74.6.1503.

Chai, G., Naldrett, A.J., 1992. The jinchuan ultramafic intrusion: Cumulate of a high-mg basaltic magma. J. Petrol. 33, 277–303. https://doi.org/10.1093/petrology/33.2.277.

Correia, C.T., Sinigoi, S., Girardi, V.A.V., Mazzucchelli, M., Tassinari, C.C.G., Giovanardi, T., 2012. The growth of large mafic intrusions: Comparing Niquelândia and Ivrea igneous complexes. Lithos 155, 167–182. https://doi.org/10.1016/j.lithos.2012.08.024.

Danni, J.C.M., Dardenne, M.A., Fuck, R.A., Ribeiro, M.J., 1973. Geologia da Extremidade Sudoeste da Serra Dourada (Goiás, Brasil). Rev. Bras. Geociências 3, 160–180.

Fuck, R.A., Pimentel, M.M., Silva, L., 1994. Compartimentaçao tectônica na porçao oriental da Provincia Tocantins, in: XXXVIII Congresso Brasileiro de Geologia, Camboriú, SBG. Sociedade Brasileira de Geolgoia, Camboriú, Brazil, pp. 215–216.

Fuck, R.A., Pimentel, M.M., Alvarenga, C.J.S., Dantas, E.L., 2017. The Northern Brasília Belt, in: Heilbron, M., Cordani, U.G., Alkmim, F.F. (Eds.), São Francisco Craton, Eastern Brazil. Springer International Publishing, pp. 205–220. 10.1007/978-3-319-01715-0_11.

Ghiorso, M.S., Sack, R.O., 1995. Chemical mass transfer in magmatic processes IV. A revised and internally consistent thermodynamic model for the interpolation and extrapolation of liquid-solid equilibria in magmatic systems at elevated temperatures and pressures. Contrib. Mineral. Petrol. 119, 197–212. https://doi.org/10.1007/BF00307281.

Girardi, V.A.V., Rivalenti, G., Sinigoi, S., 1986. The petrogenesis of the niquelandia layered basic-ultrabasic complex, central Goias. Brazil. J. Petrol. 27, 715–744. https://doi.org/10.1093/petrology/27.3.715.

Jenkins, M.C., Mungall, J.E., 2018. Genesis of the peridotite zone, stillwater complex, Montana, USA. J. Petrol. 59, 2157–2190. https://doi.org/10.1093/petrology/egy093.

Jenkins, M.C., Mungall, J.E., Zientek, M.L., Costin, G., Yao, Z., 2021. Origin of the J-M Reef and lower banded series, stillwater complex, Montana, USA. Precambrian Res. 367, 106457 https://doi.org/10.1016/j.precamres.2021.106457.

Laux, J.H., 2004. " Evolução do Arco Magmático de Goiás com base em dados geocronológicos U-Pb e Sm-Nd ." Universidade de Brasilia.

Laux, J.H., Pimentel, M.M., Dantas, E.L., Armstrong, R., Armele, A., Nilson, A.A., 2004. Mafic magmatism associated with the Goiá magmatic arc in the Anicuns region, Goiás central Brazil: Sm - Nd isotopes and new ID-TIMS and SHIMP U-Pb data. J. South Am. Earth Sci. 16, 615–630. https://doi.org/10.1016/j.jsames.2003.11.001.

Laux, J.H., Pimentel, M.M., Dantas, E.L., Armstrong, R., Junges, S.L., 2005. Two neoproterozoic crustal accretion events in the Brasília belt, central Brazil. J. South Am. Earth Sci. 183–198. https://doi.org/10.1016/j.jsames.2004.09.003.

Laux, J.H., Pimentel, M.M., Gioia, S.M.C.L., Ferreira, V.P., 2010. The Anicuns-Itaberaí volcano-sedimentary sequence, Goiás Magmatic Arc : new geochemical and Nd-S isotopic data. Geochim. Bras. 24, 13–28.

Le Vaillant, M., Barnes, S.J., Mole, D.R., Fiorentini, M.L., Laflamme, C., Denyszyn, S.W., Austin, J., Patterson, B., Godel, B., Hicks, J., Mao, Y.-J., Neaud, A., 2020. Multidisciplinary study of a complex magmatic system: The Savannah Ni-Cu-Co Camp, Western Australia. Ore Geol. Rev. 117, 103292 https://doi.org/10.1016/j.oregeorev.2019.103292.

Lesher, C.M., 1989. Komatiite-Associated Nickel Sulfide Deposits, in: Ore Deposition Associated with Magmas. Society of Economic Geologists, pp. 45–101. 10.5382/Rev.04.05.

Li, C., Ripley, E.M., 2011. The Giant Jinchuan Ni-Cu-(PGE) Deposit: Tectonic Setting, Magma Evolution, Ore Genesis, and Exploration Implications, in: Magmatic Ni-Cu and PGE Deposits<subtitle>Geology, Geochemistry, and Genesis</Subtitle>. Society of Economic Geologists. 10.5382/Rev.17.06.

Li, C., Naldrett, A.J., Ripley, E.M., 2001. Critical factors for the formation of a nickel-copper deposit in an evolved magma system: lessons from a comparison of the Pants Lake and Voisey's Bay sulfide occurrences in Labrador, Canada. Miner. Depos. 36, 85–92. https://doi.org/10.1007/s001260050288.

Lightfoot, P.C., Sage, R.P., Doherty, W., Naldrett, A.J., Sutcliffe, R.H., 1999. Mineral Potential of Proterozoic Keweenawan Intrusions: Implications of Major and Trace Element Geochemical Data from Bimodal Mafic and Felsic Volcanic Sequences of Mamainse Point and the Black Bay Peninsula, Ontario. Ontario.

Macedo, H.A.O., Della Giustina, M.E.S., de Oliveira, C.G., Praxedes, I.F., 2018. The São Luís de Montes Belos vermiculite deposit, central Brazil: Hydrothermal mineralization associated with intracontinental strike slip zones. J. South Am. Earth Sci. 88, 459–479. https://doi.org/10.1016/j.jsames.2018.08.012.

Maier, W.D., Barnes, S.-J., Ripley, E.M., 2011. The Kabanga Ni Sulfide Deposits, Tanzania<subtitle>A Review of Ore-Forming Processes</subtitle>, in: Magmatic Ni-Cu and PGE Deposits<subtitle>Geology, Geochemistry, and Genesis</Subtitle>. Society of Economic Geologists. 10.5382/Rev.17.09.

Maier, W.D., Li, C., De Waal, S.A., 2001. Why are there no major ni cu sulfide deposits in large layered mafic–ultramafic intrusions? Can. Mineral. 39, 547–556. https://doi.org/10.2113/gscanmin.39.2.547.

Maier, W.D., Barnes, S.J., Chinyepi, G., Barton, J.M., Eglington, B., Setshedi, I., 2008. The composition of magmatic Ni-Cu-(PGE) sulfide deposits in the Tati and Selebi-Phikwe belts of eastern Botswana. Miner. Depos. 43, 37–60. https://doi.org/10.1007/s00126-007-0143-5.

Manor, M.J., Scoates, J.S., Nixon, G.T., Ames, D.E., 2016. The Giant Mascot Ni-Cu-PGE deposit, British Columbia: Mineralized conduits in a convergent margin tectonic setting. Econ. Geol. 111, 57–87. https://doi.org/10.2113/econgeo.111.1.57.

Matteini, M., Junges, S.L., Dantas, E.L., Pimentel, M.M., Bühn, B., 2010. In situ zircon U-Pb and Lu-Hf isotope systematic on magmatic rocks: Insights on the crustal evolution of the Neoproterozoic Goiás Magmatic Arc, Brasília belt, Central Brazil. Gondwana Res. 17, 1–12. https://doi.org/10.1016/j.gr.2009.05.008.

Morimoto, N., 1988. Nomenclature of pyroxenes. Mineral. Petrol. 39, 55–76. https://doi.org/10.1007/BF01226262.

Mota-E-Silva, J., Ferreira Filho, C.F., Bühn, B., Dantas, E.L., 2011. Geology, petrology and geochemistry of the "Americano do Brasil" layered intrusion, central Brazil, and its Ni–Cu sulfide deposits. Miner. Depos. 46, 57–90. https://doi.org/10.1007/s00126-010-0312-9.

Mota-e-Silva, J., Filho, C.F.F., Giustina, M.E.S.D., 2013. The limoeiro deposit: Ni-Cu-PGE sulfide mineralization hosted within an ultramafic tubular magma conduit in the Borborema Province, Northeastern Brazil. Econ. Geol. 108, 1753–1771. https://doi.org/10.2113/econgeo.108.7.1753.

Mota-e-Silva, J.M., Filho, C.F.F., Bühn, B., Dantas, E.L., 2011. Geology, petrology and geochemistry of the "Americano do Brasil" layered intrusion, central Brazil, and its Ni-Cu sulfide deposits. Miner. Depos. 46, 57–90. https://doi.org/10.1007/s00126-010-0312-9.

Mungall, J.E., 2007. Crustal contamination of picritic magmas during transport through dikes: The expo intrusive suite, Cape Smith Fold Belt, New Quebec. J. Petrol. 48, 1021–1039. https://doi.org/10.1093/petrology/egm009.

Naldrett, A.J., 2004. Magmatic Sulfide Deposits, Mineralogical Magazine. Springer Berlin Heidelberg, Berlin, Heidelberg. 10.1007/978-3-662-08444-1.

Nilson, A.A., 1981. The Nature of Americano do Brasil Mafic–Ultramafic Complex and Associated Sulfide Mineralization, Goiás, Brazil. University of Western Ontário.

Nilson, A.A., Gioia, S.M.C., Pimentel, M.M., 1997. Idade Sm-Nd do Complexo Máfico-Ultramáfico Acamadado de Americano do Brasil, Goiás, E Características Isotópicas das Rochas Gnáissicas Encaixantes, in: Anais Do VI Congresso Brasileiro de Geoquímica. pp. 643–645.

Nilson, A.A., Santos, M.M., 1982. The nickel-copper sulfide deposit in the Americano do Brasil mafic–ultramafic complex, Goiás Brazil. Rev. Bras. Geociências 12, 487–497.

Nilson, A.A., 1984. Complexo Máfico-Ultramáfico de Americano do Brasil, Goiás - Geoquímica das Rochas e Implicações Petrogenéticas, in: Anais Do XXXIII Congresso Brasileiro de Geologia. Rio de Janeiro, pp. 4204–4215.

Pearce, J.A., Ernst, R.E., Peate, D.W., Rogers, C., 2021. LIP printing: Use of immobile element proxies to characterize Large Igneous Provinces in the geologic record. Lithos 392–393, 106068. https://doi.org/10.1016/j.lithos.2021.106068.

Piauilino, P.F., Hauser, N., Dantas, E.L., 2021. From passive margin to continental collision: Geochemical and isotopic constraints for E-MORB and OIB-like magmatism during the neoproterozoic evolution of the southeast Brasília Belt. Precambrian Res. 359, 105345 https://doi.org/10.1016/j.precamres.2019.105345.

Pimentel, M.M., 2016. The tectonic evolution of the Neoproterozoic Brasília Belt, central Brazil: a geochronological and isotopic approach. Braz. J. Geol. 46, 67–82. https://doi.org/10.1590/2317-4889201620150004.

Pimentel, M.M., Jost, H., Fuck, R.A., 2004. O Embasamento da Faixa Brasília e o Arco Magmático de Goiás, in: Geologia Do Continente Sul-Americano: Evolução Da Obra de Fernando Flávio Marques de Almeida. Ed. Beca, São Paulo, pp. 356–368.

Pimentel, M.M., Fuck, R.A., 1992. Neoproterozoic crustal accretion in central Brazil. Geology 20, 375–379. https://doi.org/10.1130/0091-7613(1992)020<0375.

Piña, R., 2019. The Ni-Cu-(PGE) Aguablanca Ore Deposit (SW Spain), SpringerBriefs in World Mineral Deposits. Springer International Publishing, Cham. 10.1007/978-3-319-93154-8.

Pimentel, M, Fuck, R, Ferreira Filho, C, Araujo, S, 2000. The basement of the Brasília Fold Belt and the Goiás Magmatic Arc. In: Cordani G, U, et al. (Eds.), Tectonic Evolution of South America. 1st International Geological Congress, Rio de Janeiro, pp. 195–229.

Piuzana, D., Pimentel, M.M., Fuck, R., Armstrong, R., 2003. Neoproterozoic granulite facies metamorphism and coeval granitic magmatism in the Brasilia Belt, Central Brazil: regional implications of new SHRIMP U-Pb and Sm–Nd data. Precambrian Res. 125, 245–273. https://doi.org/10.1016/S0301-9268(03)00108-6.

Putirka, K.D., 2008. Thermometers and barometers for volcanic systems. Rev. Mineral. Geochem. 69, 61–120. https://doi.org/10.2138/rmg.2008.69.3.

Ramdohr, P., 1960. Metamorfe Fölge. In: Die Erzmineralien Und Ihre Verwachsungen. Akademie-Verlag, Berlin, pp. 36–76.

Ramsay, W.R.H., Crawford, A.J., Foden, J.D., 1984. Field setting, mineralogy, chemistry, and genesis of arc picrites, New Georgia, Solomon Islands. Contrib. Mineral. Petrol. 88, 386–402. https://doi.org/10.1007/BF00376763.

Ripley, E.M., 2010. A New Perspective on Exploration for Magmatic Sulfide-Rich Ni-Cu-(PGE) Deposits. Chall. Find. New Miner. Resour. Glob. Metallog. Innov. Explor. New Discov. 10.5382/SP.15.2.06.

Roeder, P.L., Emslie, R.F., 1970. Olivine-liquid equilibrium. Contrib. Mineral. Petrol. 29, 275–289. https://doi.org/10.1007/BF00371276.

Sappin, A.-A., Constantin, M., Clark, T., van Breemen, O., 2009. Geochemistry, geochronology, and geodynamic setting of Ni–Cu ± PGE mineral prospects hosted by mafic and ultramafic intrusions in the Portneuf-Mauricie Domain, Grenville Province, QuebecGéologie Québec Contribution 8439–2008-2009-5. Geological Survey of C. Can. J. Earth Sci. 46, 331–353. https://doi.org/10.1139/E09-022.

Sappin, A.A., Constantin, M., Clark, T., 2012. Petrology of mafic and ultramafic intrusions from the Portneuf-Mauricie Domain, Grenville Province, Canada: Implications for plutonic complexes in a Proterozoic island arc. Lithos 154, 277–295. https://doi.org/10.1016/j.lithos.2012.07.016.

Shirey, S.B., Klewin, K.W., Berg, J.H., Carlson, R.W., 1994. Temporal changes in the sources of flood basalts: Isotopic and trace element evidence from the 1100 Ma old Keweenawan Mamainse Point Formation, Ontario, Canada. Geochim. Cosmochim. Acta 58, 4475–4490. https://doi.org/10.1016/0016-7037(94)90349-2.

Smith, P.M., Asimow, P.D., 2005. Adiabat-1ph: A new public front-end to the MELTS, pMELTS, and pHMELTS models. Geochem. Geophys. Geosyst. 6, 1–8. https://doi.org/10.1029/2004GC000816.

Thakurta, J., Ripley, E.M., Li, C., 2008. Geochemical constraints on the origin of sulfide mineralization in the Duke Island Complex, southeastern Alaska. Geochem. Geophys. Geosyst. 9 https://doi.org/10.1029/2008GC001982.

Yao, Z., Mungall, J.E., Jenkins, M.C., 2021. The Rustenburg Layered Suite formed as a stack of mush with transient magma chambers. Nat. Commun. 12, 1–13. https://doi.org/10.1038/s41467-020-20778-w.